Design of automated container spreader with independent Twist locking mechanism

Master Thesis

Jyotirmoy Jana

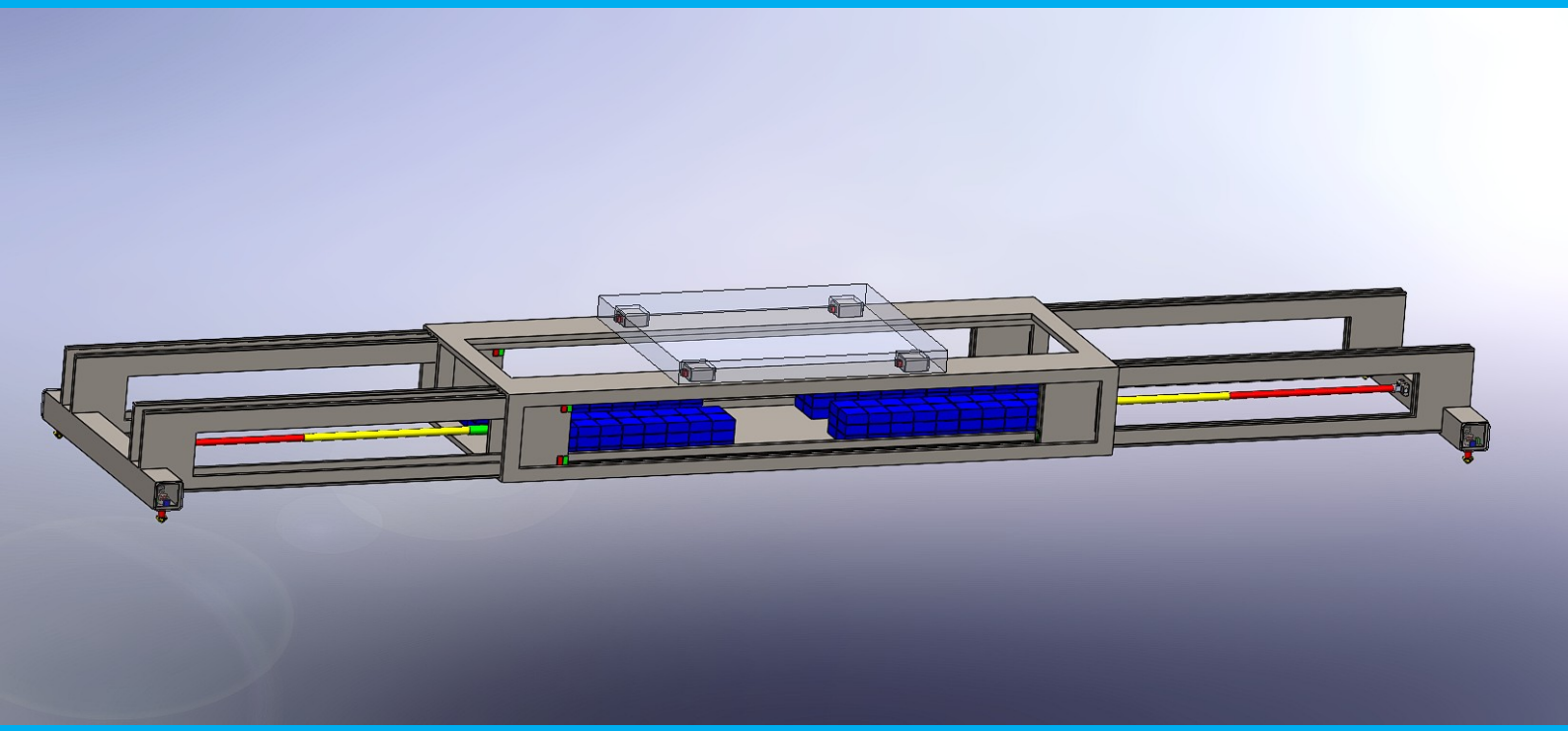

TU Delft

Design of automated container spreader with independent Twist locking mechanism

by

Jyotirmoy Jana

Master Thesis

In partial fulfilment of the requirements for the degree of

Master of Science

in Mechanical Engineering

at the Department Maritime and Transport Technology of the Faculty Mechanical Engineering
to be defended publicly on 31 March 2025, at 12:00 pm.

Student number:	5695546
MSc Track:	Multi-machine Engineering
Report Nr:	2025.MME.9047
Supervisor:	Chamod Wijesinghe
Thesis committee Chair:	Dr. Jovana Jovanova
Thesis committee Member:	Ir. W. van den Bos
Thesis committee Member:	Dr. Ir. S.P (Sebastiaan) Mulders
Date:	March 20, 2025

Acknowledgments

I would like to express my deepest gratitude to Dr. Jovana Jovanova and Chamod Wijesinghe for providing this exciting opportunity to create a meaningful impact on my academic journey at TU Delft. Their constant support and guidance has propelled me to improve my industry knowledge and gain deeper insight on the on-goings of the transportation sector during my thesis. Furthermore, I would also like to thank my peers and family for their support and understanding during my academic journey.

Abstract

The growing trend of worldwide container trade has imposed a significant strain on the technology associated with container handling. The introduction of automated equipment in terminals has proven to alleviate the issue. The process of automation is often introduced in levels classified on the basis of self-sufficiency achieved by a system. This master thesis primarily deals with identifying areas of improvement in the current process of terminal automation and generating an appropriate solution. On conducting a literature review, a particular barrier towards a higher automation level in container terminals was observed to be the spreaders utilized to handle containers. Spreaders are the primary attachment point between containers and cranes, employing rotating twist locks to engage/disengage for transportation. Currently, automatic spreaders with appropriate actuators and sensors are controlled by remote operators in advanced container terminals to manage the spreader handling processes. Some limitations are identified in these components which result in increased maintenance frequencies, higher number of failure points and rudimentary sensing capabilities. Furthermore, it is observed that the constant dependency of the automatic spreader on external sources of power reduce it's mobility and discourage it's usage in remote operations. Therefore, an iterative design method is deployed to create an enhanced spreader addressing the aforementioned issues. The final iteration of the spreader design resulted in a potential 75 percent reduction in maintenance frequency, a 50 percent reduction in the number of failure points and an integrated control algorithm comprised of advanced monitoring sensors with in-built error detection that reduce the dependency on remote operators. This improves the safety in terminals by eliminating errors occurring due to operator fatigue. An internal source of power supply is designed to improve mobility of the spreader for remote applications resulting in 20 hours of continuous operations. In combination with the independent control algorithm, this results in a potential 1 hour reduction in downtime caused by operator breaks.

Keywords: *Container handling technology, Automation levels, Container spreaders, Automated lock handling mechanism , Reduced maintenance frequency, Failure points, Improved mobility, safety*

Jyotirmoy Jana

Delft, March 20, 2025

Contents

List of Abbreviations and Nomenclature

Abrreviation	Meaning
TEU	Twenty-foot Equivalent unit
FEU	Forty-foot Equivalent unit
LOA	Level of Automation
AGV	Automated Guided Vehicle
ISO	International Standards Organization
NEN	The Royal Netherlands Standardization Institute
FEA	Finite Element Analysis
CAD	Computer Aided Design
FOS	Factor of Safety
BLF	Buckling Load Factor
g	Gravitational constant
C_d	Aerodynamic co-efficient
ρ	Air density
v	Wind velocity
ϕ	Dynamic hoisting co-efficient
τ	Shear stress
ϵ	Strain
δ	Deflection
MPa	Mega Pascal
W	Watts
J	Joules
V	Volts
A	Ampere

List of Figures

List of Tables

1. Introduction

The rapid growth of globalized industrial trade and international supply chain processes have caused a significant strain on the transportation industry across the world. Standardized transportation techniques have gained massive popularity in the past few decades mainly due to higher efficiency and lower costs. One such technique was the introduction of containerization in 1956. Containers are available in two sizes, Twenty-foot Equivalent Units (TEUs) and Forty-foot Equivalent Units (FEUs) and container transportation is responsible for about 60 percent of the total trade value worldwide [1].

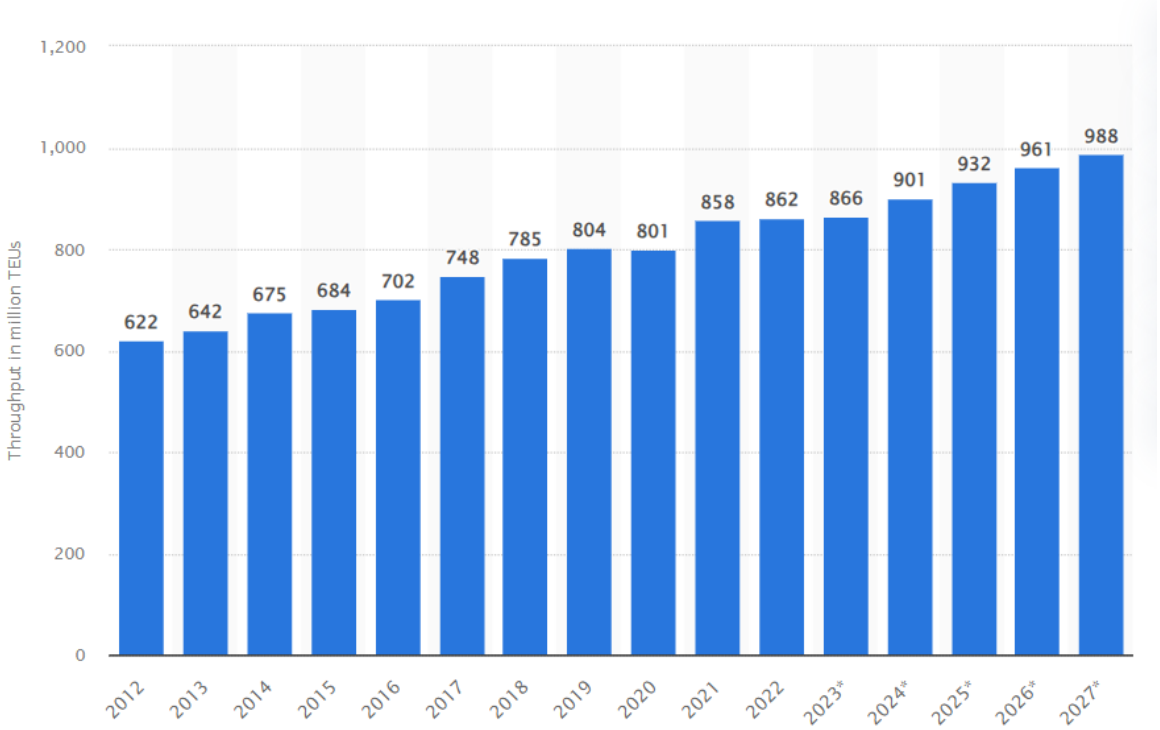

Figure 1.1: Trends in global container trade

From Figure 1.1, it can observed that 901 million TEUs were handled globally in 2024, with projections looking to cross the 1 billion mark over the forthcoming years [2]. This progressive trend calls for advancements in container transportation technology and research in the same has become the forefront of innovation for the transport industry. Moreover, the ever-growing necessity of operational safety, efficiency and cost management has motivated authorities and researchers to investigate innovative approaches for container handling and transportation. One such method is known to be automation of equipment utilized in the container terminal.

1.1. Automation in transportation

Automation in terms of engineering can be defined as the process of replacing human operated tasks in a system with suitable machinery and equipment [3]. This process is usually categorized in levels based on the capability of self-sufficiency achieved by a particular automated system.There are numerous methods of categorizing levels of automation in the industry, however, for the scope of this thesis, the proposed levels are declared based on the research conducted by Vagia et. al. where the authors have attempted to summarize a variety of proposed taxonomies of automation and compile them in a suitable manner. This summarized taxonomy of Levels Of Automation (LOA) is listed as follows:
Level 1: Manual control where no computer assistance is provided.
Level 2: Decision proposal stage where computer offers some decisions to the operator and the operator is responsible to decide and execute.
Level 3: Human decision select stage where the human selects one decision and the computer executes.
Level 4: Computer decision select stage where the computer selects one decision and executes with human approval.
Level 5: Computer execution and human information stage where the computer executes the selected decision and informs the human.

Level 6: Computer execution and on call human information stage where the computer executes the selected decision and informs the human only if asked.
Level 7: Computer execution and voluntarily information stage where the computer executes the selected decision and informs the human only if it decides to.
Level 8: Autonomous control stage where the computer does everything without human notification, except if an error that is not into the specifications arrives. In that case the computer needs to inform the operator [3].
In the context of container transportation, numerous advancements in automation technologies can be observed. These advancements are primarily in the form of automated handling equipment deployed at container terminals.

(a) Automated Rail-mounted Gantry Crane

(b) Automated Guided Vehicle (AGV)

Figure 1.2: Automated container handling equipment

Implementing automated equipment at the terminal has proven to boost safety via reducing the requirement of manual operators at the terminal. For example, introduction of equipment like AGVs observed in Figure 1.2 have significantly improved safety at the terminals via the use of appropriate sensors and reduced labor costs by eliminating human-operated machinery like trucks or forklifts. Moreover, the probability of successful operations is improved since the risk of human error is minimized by utilizing AGVs [4]. However, it is observed that the some tasks in the container handling process still massively rely on control by operators and require considerable manual oversight. Therefore, a literature assessment is conducted to explore a scope of improvement.

1.2. Literature assessment

On assessing all currently available container handling equipment and their offered automation capabilities, a common factor that proved to be a barrier towards a higher LOA was the handling of spreaders. Spreaders are equipment utilized as the main attachment point between a container and other handling equipment such as cranes. They lock onto a container using twist locks and enable the crane to successfully lift and transport a container to it's desired location [5]. Currently, a spreader can be classified as follows: Manual, Semi-automatic and Fully automatic.

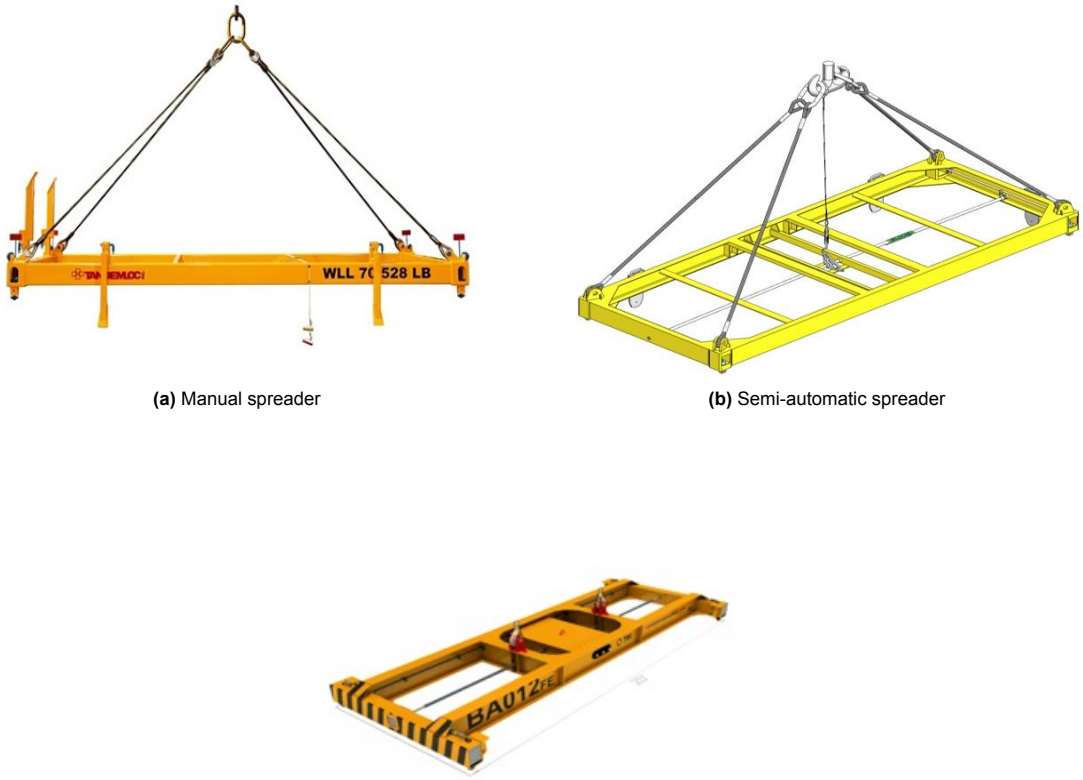

(a) Manual spreader

(b) Semi-automatic spreader

(c) Fully-automatic spreader

Figure 1.3: Line-up of currently available container spreaders

Manual spreader: The process of locking/unlocking a spreader onto a container is entirely manual. An operator is responsible for confirming spreader position at all times along with utilizing handling rods to manually lock a spreader onto the container. This is a conventional approach which requires a lot of handling time and risks the safety of the operators in the terminal [6].

Semi-automatic spreader: The spreader uses a slacking mechanism for automatic locking/unlocking. After landing on a container, the crane operator fully slacks the spreader onto the container for engagement. At the destination, the spreader is slacked again to unlock the bayonets. This system eliminates manual locking/unlocking but requires a skilled on-site crane operator and ground staff for position confirmation [7].

Fully-automatic spreader: The locking/unlocking system is controlled remotely via a battery-powered electric mechanism. Appropriate sensors and actuators are utilized to identify position and to initiate locking/unlocking. This eliminates the need for on-site crane operators and ground staff but still requires a remote operator to perform every required action [8].

Automated terminals utilize a fully automatic spreader where a remote operator instructs the spreader to perform each operational task. Based on the predefined LOA from Section 1.1, a fully automatic spreader can be classified at level 3, where the human selects one decision and instructs the equipment for execution. These remote operators work in rotating shifts of 8 hours with a 30 minute break entitled to the operator during each shift [9]. Moreover, these operators are bound to experience fatigue after sitting in one place for several hours and this could lead to risk of accidents due to human error.

Figure 1.4: A remote operator controlling an automatic spreader

In terms of twist locking mechanism, the automatic spreaders offer the capability of remote rotation of twist locks via an actuated drive linkage connected to each shaft of the locks. While lowering, the operator can identify sufficient engagement between the spreader and container via landing pins attached at the bottom of spreader frame connected to a limit switch to relay confirmation. A successful rotation of twist locks is confirmed via another pair of limit switches attached above the rotating shaft [10]. This mechanism offers decent control over the locking process but some limitations are identified.

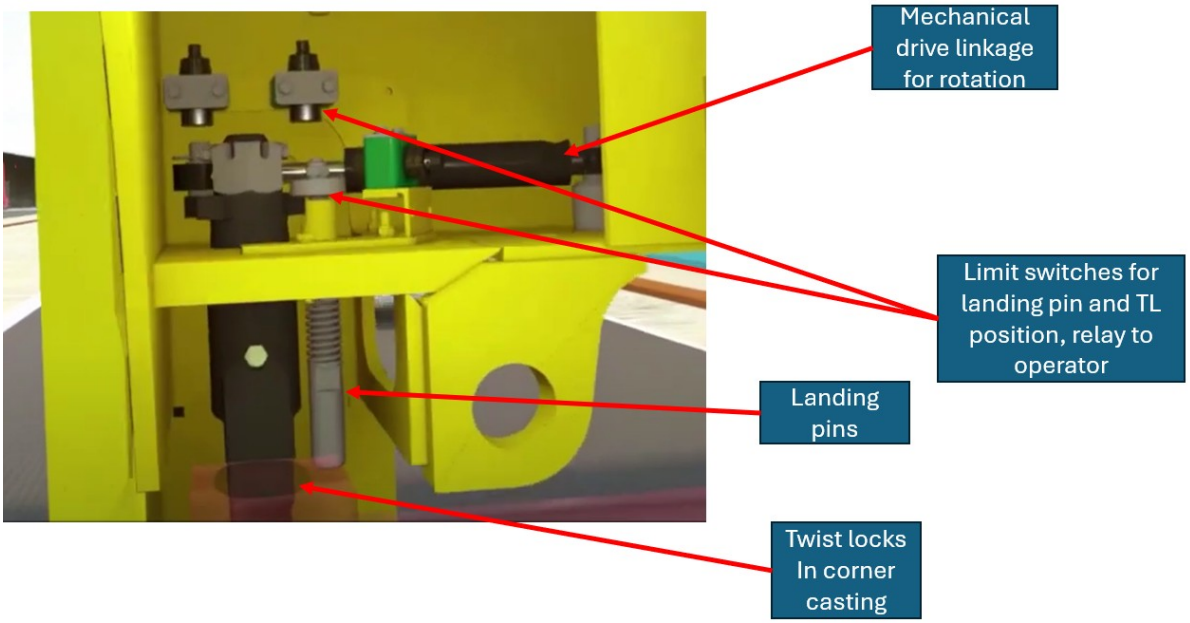

Figure 1.5: Mechanism for locking/unlocking in automatic spreaders

On observing the locking mechanism from Figure 1.5, following are some limitations observed:

Landing pins utilized for container detection constantly require physical contact for a successful detection. This can potentially damage the pins over time and cause frequent maintenance or replacements leading to increased down time of spreader. It is estimated that these pins require maintenance every 3 to 6 months for inspection and alignment verification [11]. Moreover, the accuracy of the landing pins maybe affected if there are surface irregularities present at the corner casting of the container.

Limit switch sensors used for confirmation of spreader engagement are fairly primitive in their function and cannot facilitate continuous monitoring of operations, not suited for higher automated control. Moreover, they are prone to mechanical degradation due to extensive contact, misalignment and are considered as one of the key failure points in automatic spreaders [12].

Drive linkage used for rotation of twist locks comprises of multiple moving parts leading to higher number of failure points. Typically, the automatic spreader utilizes an electric motor at each extendable arm connected to a gearbox which translates two couplers, each attached to additional pivot rods for rotation of locks [13]. Therefore, the total number of moving parts in this configuration amounts to 8, potentially increasing the probability of breakdowns. Moreover, since the drive linkage is connected to a central actuating mechanism, the spreader lacks independent control over each corner.

In addition to the limitations observed in the twist locking mechanism, the frame of automatic spreaders is analyzed to identify any areas of improvement. There are numerous iterations of automatic spreader frames available, with most offering dual-size lifting abilities, i.e., both FEU and TEU containers. This is achieved by utilizing actuated extension arms to provide the extra length required for FEU containers. The frame is designed to withstand all operational challenges including load handling capacity and resistance to the harsh environment usually experience at container terminals [14].

Figure 1.6: Automatic dual-size spreader by BROMMA

These designs are inherently quite capable and optimized, however, some potential scope of further advancements is observed as follows:

External power supply: They require a constant source of external power supply as there is no space for an internal source of power for operations. This limits the use of the spreader in mobile operations.

Fixed attachment: Spreader frame have a fixed provision for insertion of locks to attach onto secondary equipment. The attachment/detachment of the spreader always relies on an external source and this could be potentially dangerous in case of emergencies where power supply is unstable.

The purpose of this master thesis is to introduce an enhanced spreader design that addresses these limitations and potentially improves the safety, mobility and automation capability while reducing maintenance requirements and potential failure points. First of all, it is necessary to define a structured methodology for execution.

2. Methodology

To solve any engineering problem, it is essential to devise a structured course of action. For design oriented problems, using an iterative design process is a widely acceptable method of innovation. Iterative design allows the user to generate an initial concept based on predefined product requirements, and then enters the concept into an iterative cycle of constant tweaking via testing and evaluation until the final concept design matches the requirements [15]. This final iteration of the process is then proposed for deployment, as observed in Figure 2.1.

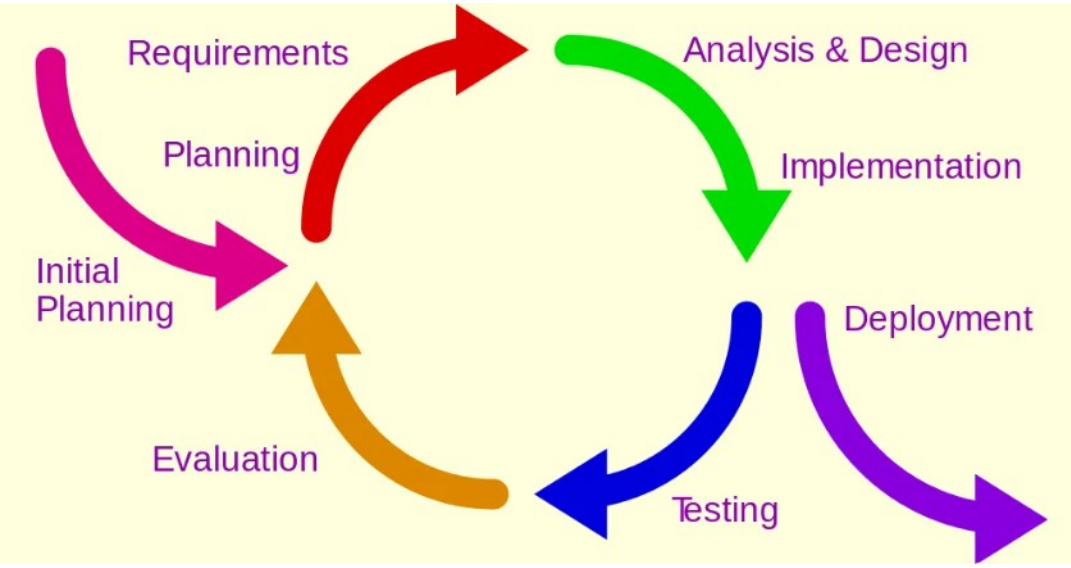

Figure 2.1: Schematic of an iterative design process

2.1. Product Requirements

A successful incorporation of the iterative design process initially requires identification of all the operational requirements to be fulfilled by the final iteration of a potential design. These requirements are necessary to ensure feasibility of the potential design and will be the reference point for each iteration. Following are the expected requirements to be satisfied by the new spreader design:

Sr. No.	Product requirements	Explanation
1	Dimensional feasibility	Capable of lifting FEU and TEU containers
2	Load Capacity	Capable of handling all static and dynamic loads during operations
3	Environmental exposure	Withstand harsh winds, exposure to dust, moisture and corrosion experienced at terminals
4	Safety and standards compliance	Compliant to NEN EN 15056: Cranes- Requirements for container spreaders [16]
5	Automated locking/ unlocking	Independent locking/unlocking mechanism
6	Compatibility	Easily attachable/detachable from secondary handling equipment
7	Accessibility	Easy access to components for maintenance/ replacement
8	Independent operations	Internal power supply available

Table 2.1: Product requirements for automated spreader

The requirements defined in Table 2.1 are referred at the end of the iterative cycles to verify if the spreader design is fulfilling it's prerequisites. If it fails to satisfy any of the requirements, the iteration is restarted with the appropriate corrective measures.

2.2. Initial concept

Based on the aforementioned product requirements, a list of initial concept suggestions is generated. The dimension and weight of the containers that need to be transported by the spreader are regulated by the International Standards Organization (ISO), specifically ISO 668: freight containers — Classification, dimensions and ratings [17]. The declared properties for both FEU and TEU containers are tabulated as follows:

Property	TEU	FEU
Dimensions	Length: 20 feet (6.05m) Width: 8 feet (2.43m) Height: 8'6" (2.59m)	Length: 40 feet (12.2m) Width: 8 feet (2.43m) Height: 8'6" (2.59m)
Max. payload	28,200 kgs	28,800 kgs

Table 2.2: TEU and FEU dimensions and payload capacities as per ISO 668

The initial concept suggestions are as follows: On observing fully automatic spreaders like the one in Figure 1.6, a common trend was observed to be the use of extendable arms to enable dual-size lifting of TEU and FEU containers. Hence, a suitable suggestion would be to **split the spreader frame assembly into two parts**, the mainframe and the extendable arms. Moreover, to avoid complicated extension mechanisms, the mainframe can be dimensioned in reference to TEU dimensions. This will allow ample space for storing the arms when not in use and to house other components required for operations, along with space for internal power supply. The maximum allowable payload of FEU containers is 28,800 kgs. However, a sample rated capacity of the spreader is considered according to Annex A of NEN 15056, which indicates a design capable of **handling up to 40000 kgs**. The structure of spreader should be able to withstand all the imposed stresses along with the harsh environments experienced at the terminals. An initial analysis suggests the use of **steel alloys** as the material of choice for the spreader frame, primarily due to its excellent strength, durability and corrosion resistance properties [18]. To ensure ease of accessibility, it is suggested to consider an **open frame design** via strategic cutouts that improve access to internal components while maintaining structural integrity. All the product requirements and initial concept suggestions have been defined for designing the automated spreader and iterative cycles are initiated for analysis.

2.3. Iterative cycle breakdown

To simplify the iterative process, two cycles called **structural integrity** and **operational feasibility** are utilized for analysis of the spreader. The structural integrity cycle ensures that the spreader frame is capable of withstanding all operational challenges without experiencing failure under pressure. An initial design for the frame is generated using SolidWorks where it will be modeled as a CAD assembly of all the necessary parts essential for operations. Any required design modification will be first implemented on SolidWorks and then pushed forwards for testing and evaluation. The integrity is tested via Finite Element Analysis (FEA), which is available on Solidworks as a simulation add-in. FEA is a computational method utilized to examine the behavior of physical systems by dividing a continuous component/assembly of components into smaller finite elements. These elements are combined to form a mesh of the entire component or assembly. This technique allows for better analysis of the component assembly [19]. The testing parameters will be formulated using appropriate mathematical formulas and numerical methods. The results from the FEA are compared to the safety standards mentioned in Table 2.1 to verify competence. Once the frame of the spreader is feasible for utility, the operational feasibility cycle begins by defining all the actuators and sensors required for spreader operations. To integrate these components in order to achieve higher levels of automation, a structured control algorithm is simulated on MATLAB simulink, a tool used for simulation programming. The control algorithm is tested for evaluating feasibility of chosen apparatus of components. Finally, after completing both cycles,the resultant iteration is compared to the product requirements to check compatibility.

2.4. Adapted iterative design process chart

A process chart is created with suitable adaptations for designing a container spreader. This chart establishes a structured flow for the entire process with the possibility of continuous improvement at each stage. It is visualized as follows:

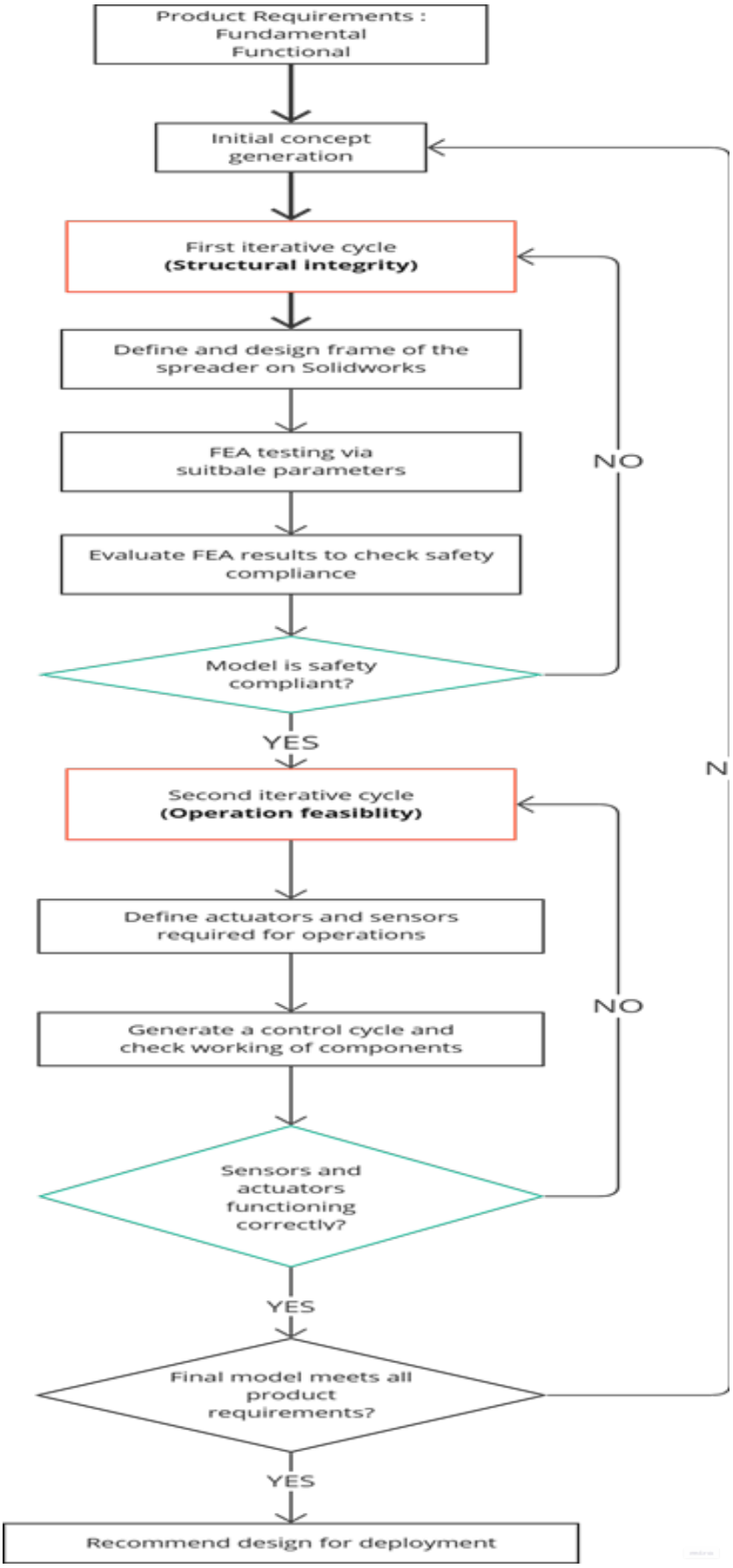

Figure 2.2: Adapted iterative chart for spreader design

3. Iterative cycle for structural integrity

This cycle of iterations deals with verifying structural integrity of the optimized spreader design during operations via Finite Element Analysis (FEA). Firstly, a suitable spreader frame is designed in Section 3.1 according to the requirements and suggestions mentioned in Section 2.2. Secondly, suitable parameters required during FEA testing are defined in Section 3.2. Thirdly, a simulation study is setup with required testing parameters in Section 3.2.2. Once the simulation test is complete, the generated results are evaluated to verify competence according to safety standards for container handling equipment in Section 3.2.3. If the resultant values do not fall within the recommended range, the entire process is repeated with a modified design.

3.1. Design of spreader frame

The spreader frame will house all necessary components required for operations. Hence, the design of frame should consider adequate dimensioning along with suitable structure and material for ensuring reliability and feasibility. The frame is designed in three stages/parts: the mainframe, frame of the extendable arms and the twist locks used for attachment to containers. Subsequently, the connection between each part is explained.

Mainframe: It can be regarded as the main body of a spreader as it is utilized for attaching the spreader onto secondary handling equipment such as cranes along with housing the extendable arms and all the components required for operations. Therefore, it is necessary to design a sturdy and rigid frame with appropriate dimensions capable of withstanding all loads and environmental challenges experienced by a spreader. Referencing the initial concept considerations observed in Section 2.2, a CAD model of the mainframe is generated on SolidWorks:

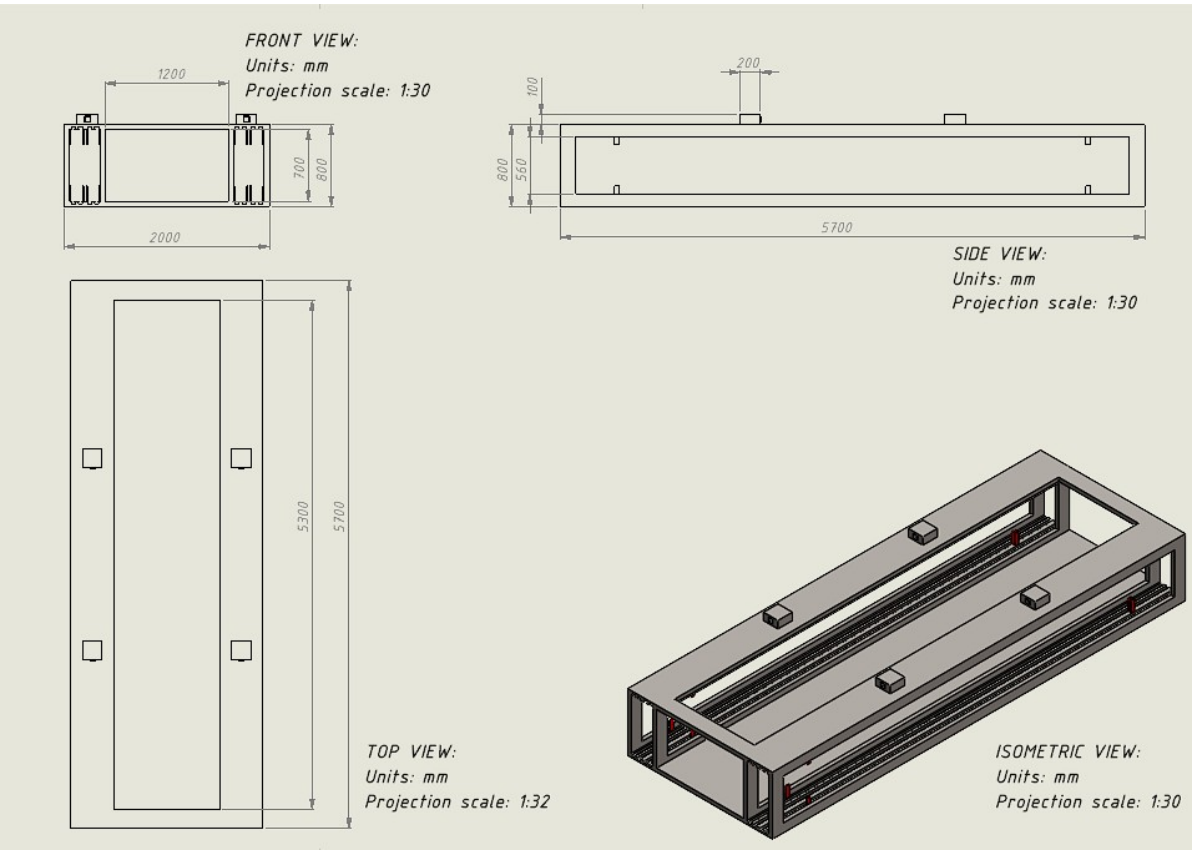

Figure 3.1: Mainframe of spreader

As observed from Figure 3.1, the mainframe is designed in reference to TEU dimensions such that the arms will not require extension while lifting a Twenty-foot container. It consists of two rail provisions along it's length to store the extendable arms along with four housing boxes to accommodate an in-built release mechanism. The design accounts for improved accessibility for components via minimal usage of base plates and strategic cutouts in the frame.

Frame of extendable arms: The extendable arms are utilized to facilitate FEU container lifting. In a fully extended position, these arms will experience the maximum stress from container loads along with potential wind forces at the terminal. Moreover, the arms also need weigh as minimal as possible to be feasible for actuated extension. Therefore, it is essential to design a sleek yet durable arm which can withstand the load of the container in a limited structural weight. A CAD model of the frame of extendable arms is generated as follows:

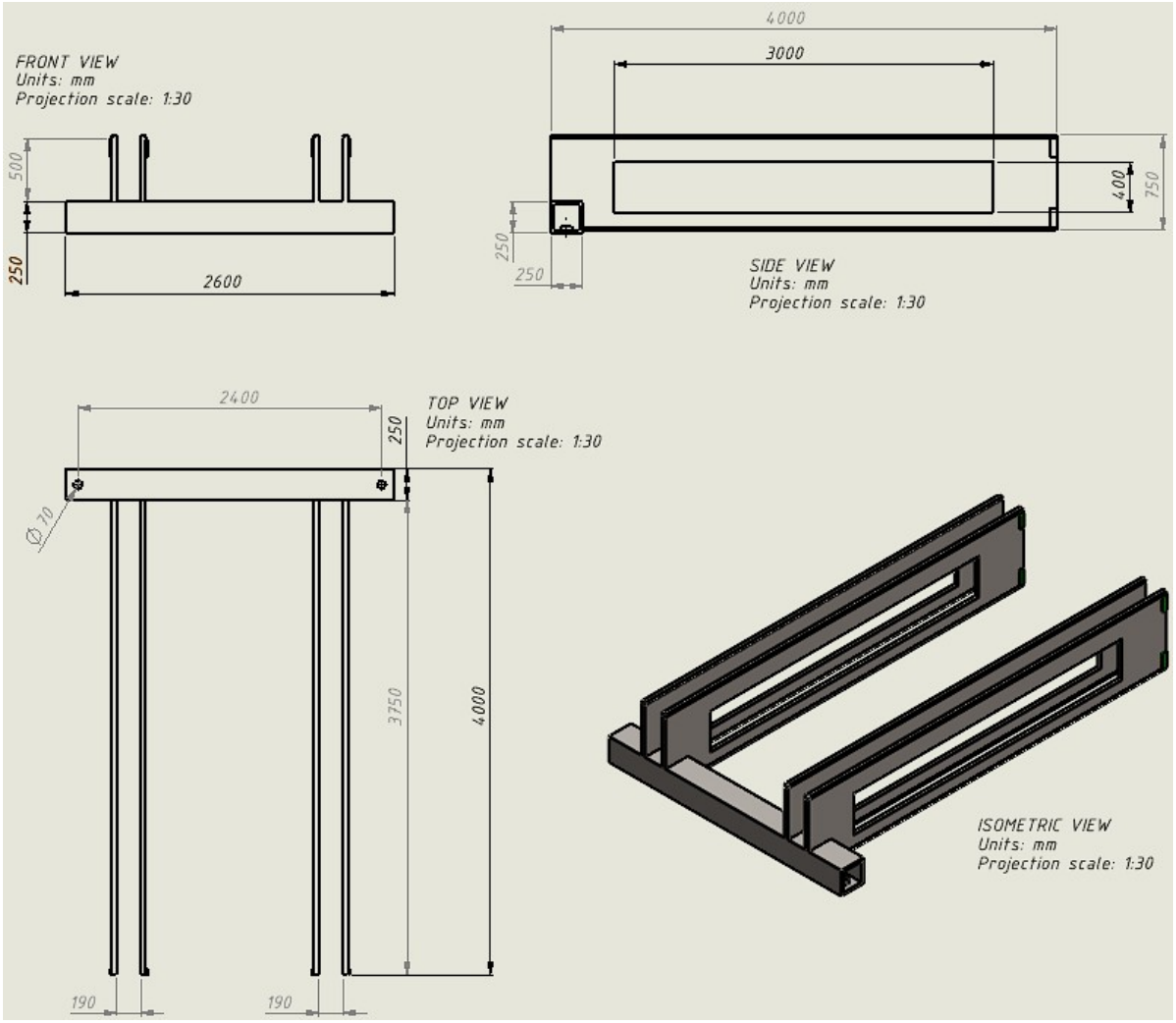

Figure 3.2: Frame of extendable arm

As observed from Figure 3.2, the frame of extendable arms comprises of connection beams with suitable length to facilitate FEU lifting. Each connection beam has guide extensions to slide onto the rails installed on the mainframe. A hollow square beam dimensioned as per container width is connected at the end of the arms. The square beam shall house the twist locks necessary for engagement to a container.

Twist locks: Twist locks are an essential component in the spreader assembly as they are the primary contact between a container and the spreader. They are inserted into the corner castings of a container and then rotated to lock/unlock onto the container during transport. The design of twist locks is heavily influenced by regulations on corner casting dimensions as per ISO 668: freight containers — Classification, dimensions and ratings container dimensions [17]. It is preferable to strictly adhere to the standard dimensions and tolerances used for the corner castings during design . Therefore, an appropriate twist lock head is modeled as follows:

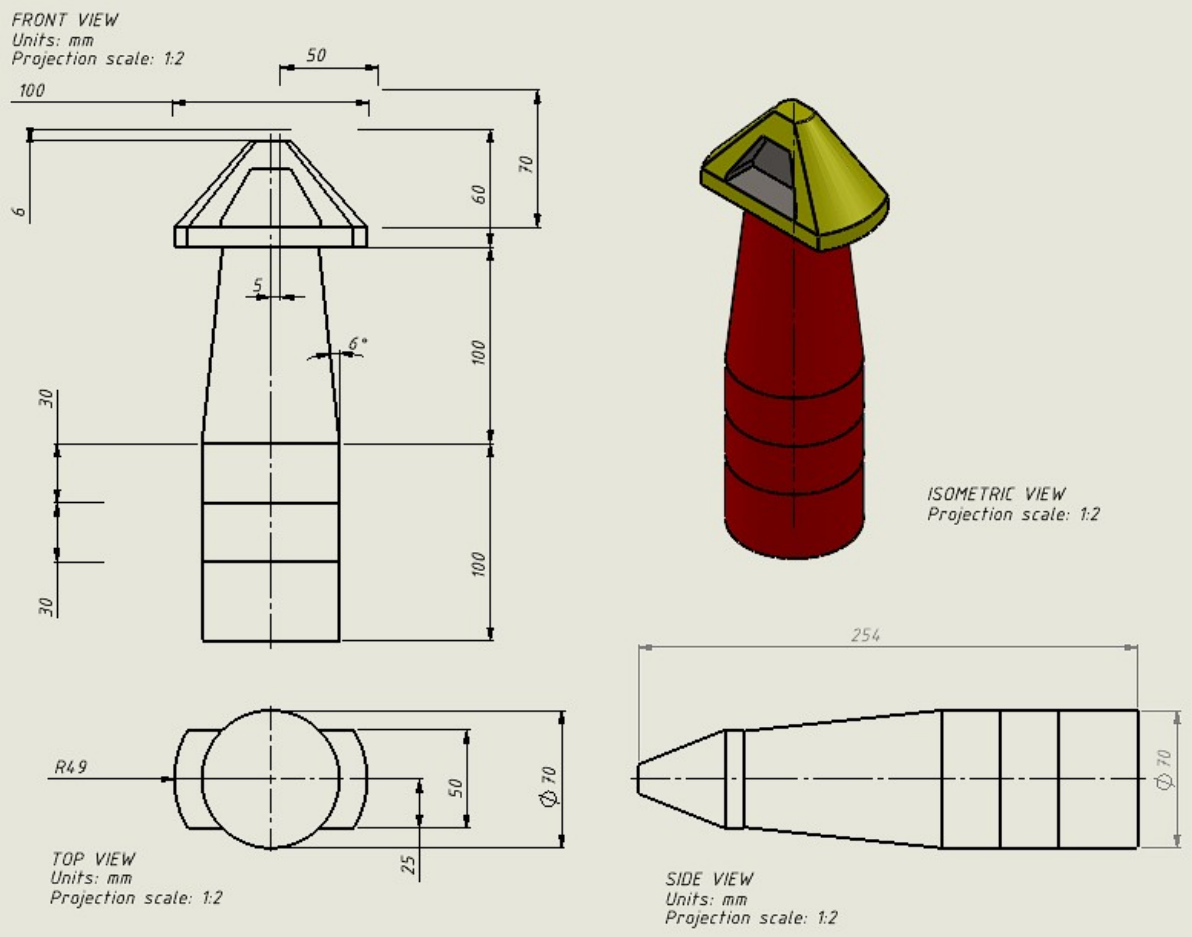

Figure 3.3: Twist lock head as per ISO standard dimension with appropriate connecting shaft

As observed in Figure 3.3, the head of the twist lock is dimensioned as per the declared ISO dimensions of container corner castings. The head is attached to a connecting shaft of suitable diameter and length for installation onto the extendable arms. Now that each part of the spreader frame is defined, it is important to understand the connections in-between them to fully establish a functional frame assembly.

Connection between mainframe and arms:
A rail-guide connection is used to attach the spreader arms to the mainframe. The mainframe is designed with rails installed on both top and bottom base plates. The connection beams of extendable arms possess guide extensions along their entire length to allow better load distribution and structural support, as observed in Figure 3.4.

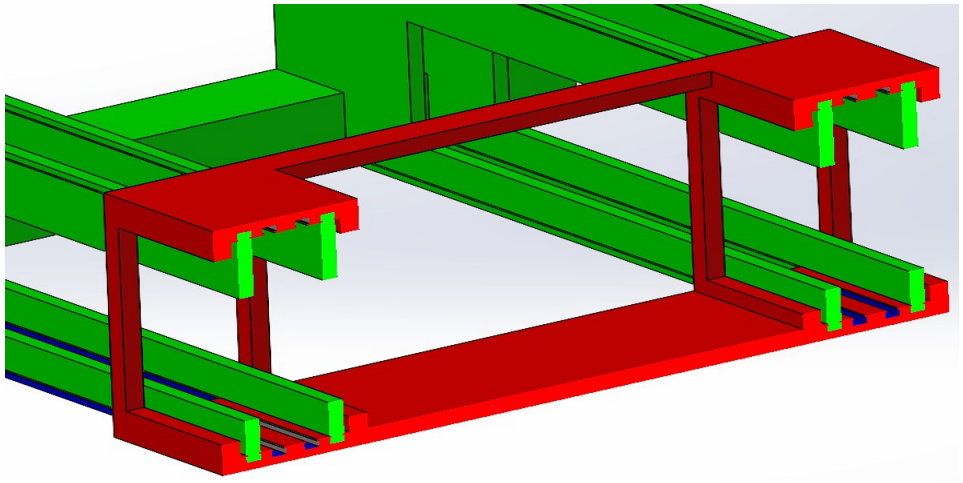

Figure 3.4: Sectional view of rail guide connection: Spreader arm (green) and mainframe (red)

To prevent the arms from falling out of the mainframe during operations, custom stop blocks are installed on both mainframe and spreader arms at the end of the designated travel lengths. Although the actuating mechanism for extension usually possesses an in-built braking system, it is essential to account for brake failure and hence emergency stop blocks are necessary for additional safety. They are visualized as follows:

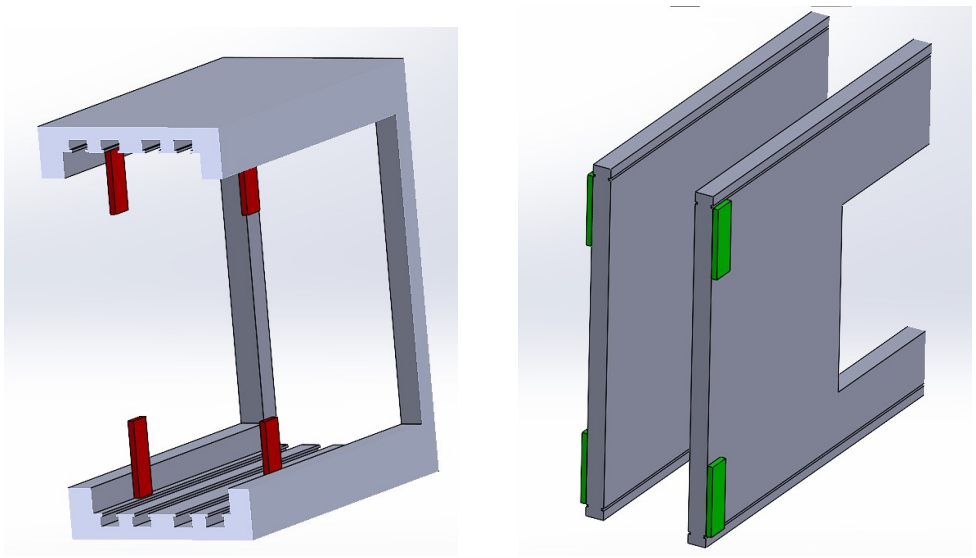

(a) Stop blocks on mainframe **(b)** Stop blocks on spreader arm

Figure 3.5: Sectional view: stop blocks on spreader arm (green) and mainframe (red)

As observed from Figure 3.5, the stop blocks are positioned on the mainframe to allow the extendable arms to reach only the required position for FEU lifting and not more. It is also necessary to ensure that there is no interference between both arms when they are stored inside the mainframe. This is achieved by utilizing rails of varying widths on the mainframe. One of the arms has wider pair of connection beams than the other so that it enclose over the narrower beam pair during storage. Therefore, each arm uses a different rail from the mainframe as it's connection and consequently prevents interference, as observed in Figure 3.6.

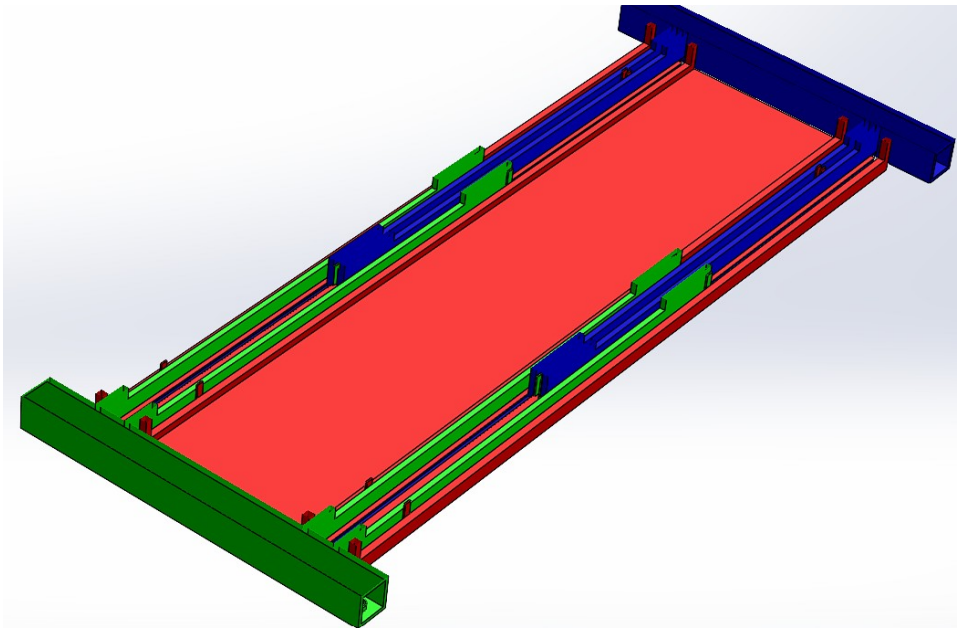

Figure 3.6: Sectional view: wider arm (green) enclosing narrower arm (blue) inside the mainframe (red) during storage

Connection between arms and twist locks:
The connection between twist locks and the frame of extendable arms has to account for a rotational degree of freedom while maintaining a rigid connection to the frame. Hence, a bearing connection is deemed to be the ideal choice of attaching the twist locks to the arm frame. The bearings will allow for rotational freedom while handling all static and dynamic loads experienced during operations. They are also resistant to environmental challenges as they can be covered using protective sealing [20].

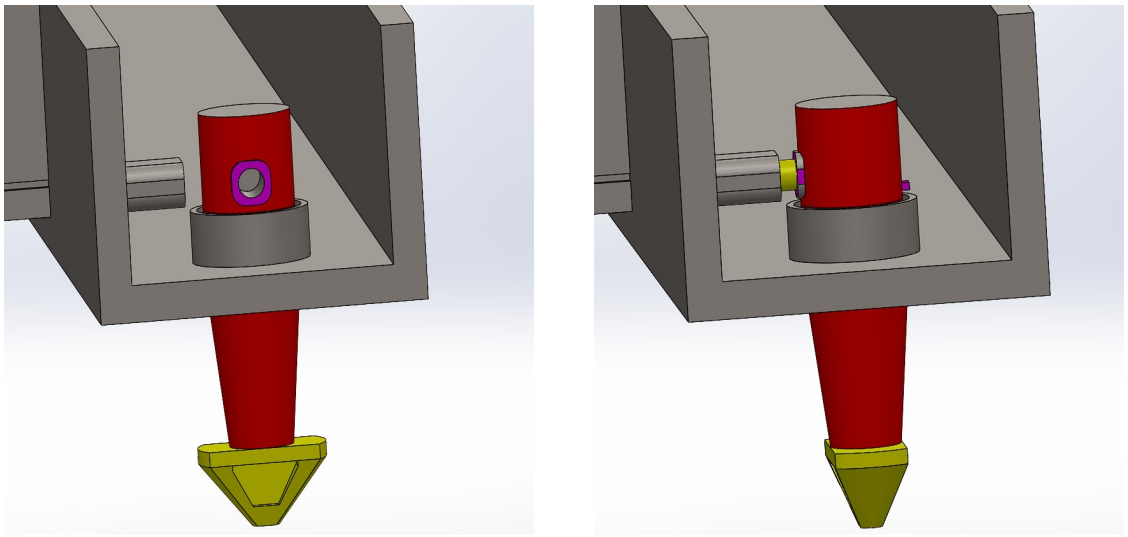

(a) Twist lock in unlocked position

(b) Twist locks in locked position

Figure 3.7: Sectional view: Bearing connection with actuated locking pin used to secure twist locks during transport

To further safeguard operations, an actuated locking pin is inserted into the connecting shaft of the twist lock when the spreader is engaged to a container during transport, Figure 3.7. This ensures that the twist locks will not back-drive during operations due to moving load of the container.

Connection between mainframe and secondary equipment:
To facilitate an in-built quick release mechanism for attaching/detaching a spreader onto secondary equipment, an intermediate connection plate is introduced. At the bottom, this plate will have insertion slots of appropriate dimensions as per the housing boxes and the telescopic extensions designed in the mainframe. The top of connection plate can be modified to suit the attachment method chosen for the secondary equipment, for example, pulleys, hooks or fixed attachment. The release mechanism can be visualized as follows:

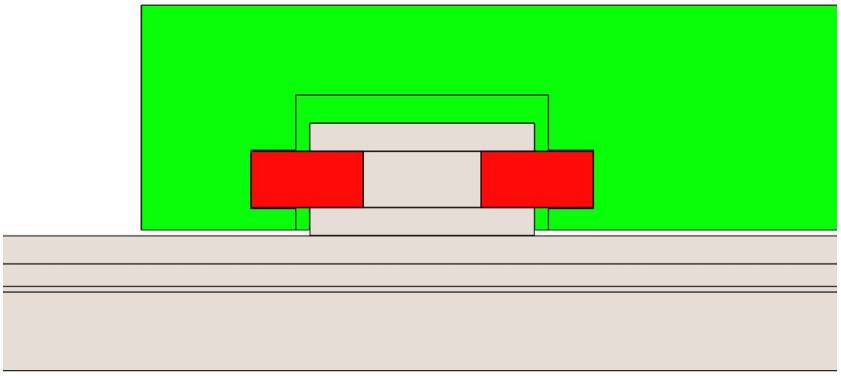

Figure 3.8: Sectional side view: Connector plate(green) with actuated extensions(red) inserted to lock the plate and mainframe

To prevent any unexpected lateral movement of the extensions during transport, a pair of locking pins are introduced in the telescopic extensions for redundancy. They wedge into the connection plate laterally and secure the spreader attachment to secondary equipment, as observed in Figure 3.9.

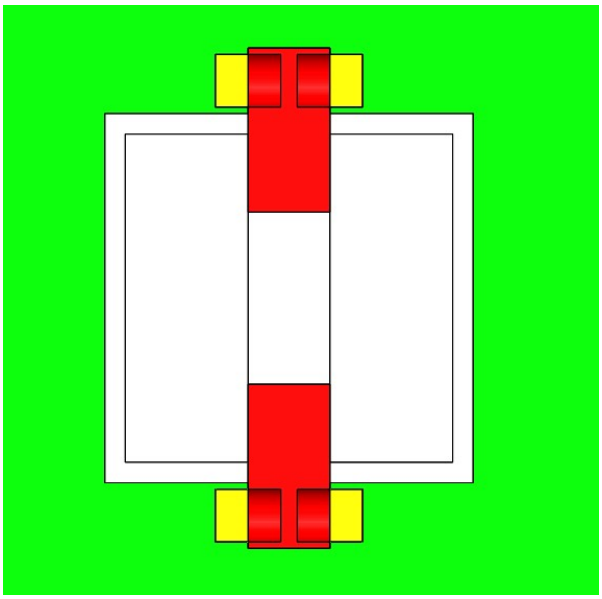

Figure 3.9: Sectional top view: Locking pins (yellow) wedged into the connector plate (green)

The entire spreader frame assembly is now established with each part and connection fully examined. This frame will be thoroughly tested for confirming structural integrity during operations. The tests are carried out via the method of Finite Element Analysis (FEA).

3.2. Finite Element Analysis (FEA)

FEA is divided into three stages, called pre-processing, analysis and post-processing. The pre-processing stage involves defining all operational parameters relevant for analyzing the spreader frame. Once all relevant parameters are identified, a suitable test case is setup in the analysis stage to observe the behaviour of the spreader in it's operational environment. Finally, the results of the test case are evaluated for verifying structural integrity in the post-processing stage.

3.2.1. Pre-processing

The operational parameters are the properties that need to be defined for a realistic analysis of the spreader frame. They are the foundational elements used to emulate the real-world working conditions of the spreader. They can be classified as geometries and meshing, material properties, boundary conditions, loads and element selection.

Geometry and meshing: The orientation of the spreader frame chosen for analysis needs to impose the maximum possible damage on the frame to thoroughly analyze the integrity of the structure. The maximum bending force is exerted when the spreader arms are fully extended for FEU container lifting. Therefore, a fully-extended arm position is a suitable geometric orientation for analysis. The twist locks are positioned in their locked orientation with locking pins latched into connecting shafts since that is when the load from containers is experienced by the frame. The release mechanism is in it's fully extended orientation to emulate attachment to the connector plate.

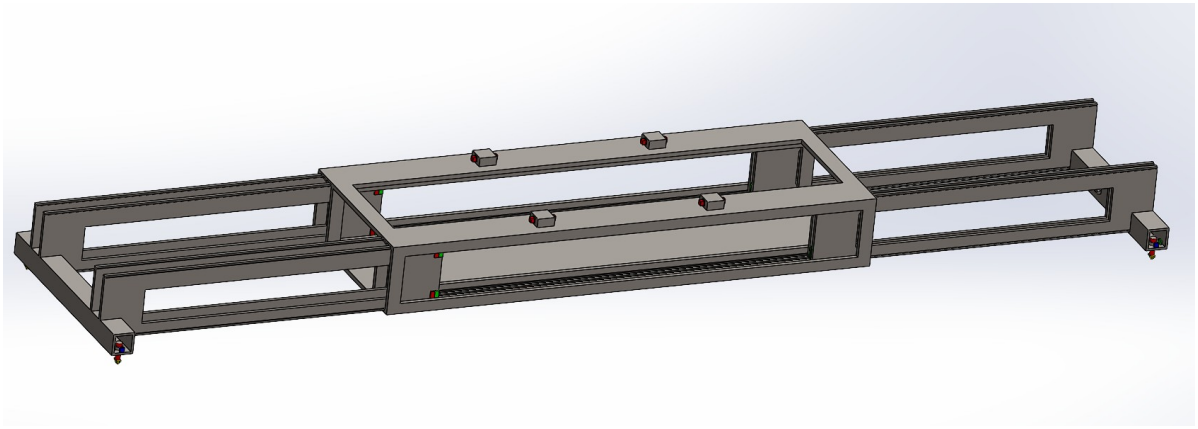

Figure 3.10: Spreader orientation chosen for FEA

On finalizing the geometrical orientation observed in Figure 3.10, the model is discretized into smaller elements to approximate the continuous model into a finite assembly of elements. This discretization can be observed in the form of a meshed assembly as follows:

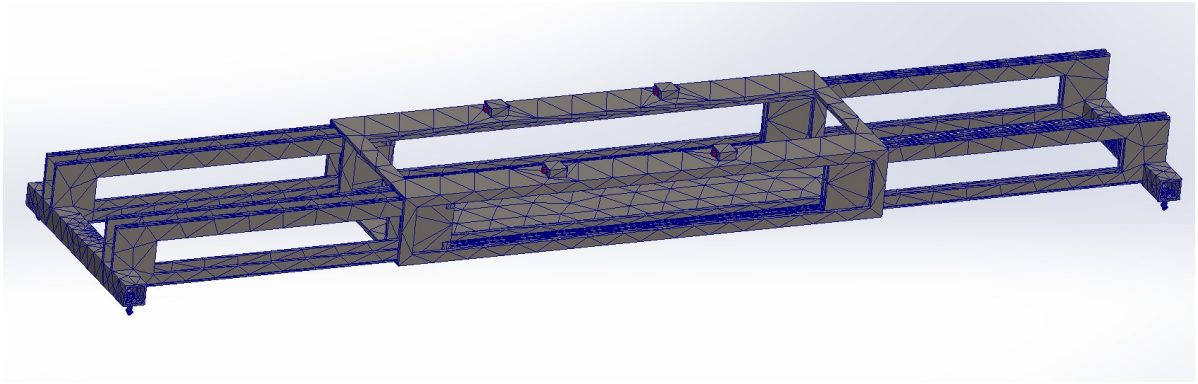

Figure 3.11: Meshed spreader frame assembly

As observed from Figure 3.11, the frame is discretized into a blended curvature-based mesh in Solidworks simulation panel. This feature automatically adapts the element size based on the local curvature of the geometry chosen.

Material properties: As per the initial concept suggestions mentioned Section 2.2, the material of choice for the spreader frame is an alloy of steel, mainly due it's strength, durability and corrosion resistance. Currently, container spreaders are primarily made of high-strength steel due to their durability, load-bearing capacity and deformation resistance [21]. Therefore, on exploring the available steel alloys in SolidWorks material library, a Stainless Steel (SS) alloy is opted as the material of choice applied on the mainframe and the extendable arm frame, mainly due to it's higher tensile and yield strengths. The properties of this alloy are listed as follows:

Property	Value	Units
Elastic Modulus	210000	N/mm^2
Poisson's Ratio	0.28	N/A
Shear Modulus	79000	N/mm^2
Mass Density	7700	kg/m^3
Tensile Strength	723.8256	N/mm^2
Yield Strength	620.422	N/mm^2
Thermal Expansion Coefficient	1.30E-05	/K
Thermal Conductivity	50	W/(m·K)
Specific Heat	460	J/(kg·K)

Table 3.1: Material properties of mainframe and frame of extendable arms

Twist locks are usually made of galvanized steel to allow protection against harsh weather and structural rigidity [22]. Therefore, the properties of this steel are imported from the SolidWorks library and applied in the simulation panel:

Property	Value	Units
Elastic Modulus	200000	N/mm^2
Poisson's Ratio	0.29	N/A
Mass Density	7870	kg/m^3
Tensile Strength	356.9007	N/mm^2
Yield Strength	203.9432	N/mm^2

Table 3.2: Material properties of Twist locks

Boundary conditions: The boundary conditions are a crucial aspect during FEA as they dictate how the model is going to interact with the operational environment and external factors which involves defining all constraints on the model assembly. The primary constraint on the spreader assembly is the fixture of the mainframe release extensions into the connection plate that can be further attached to equipment such as cranes. This constraint can be implemented as follows:

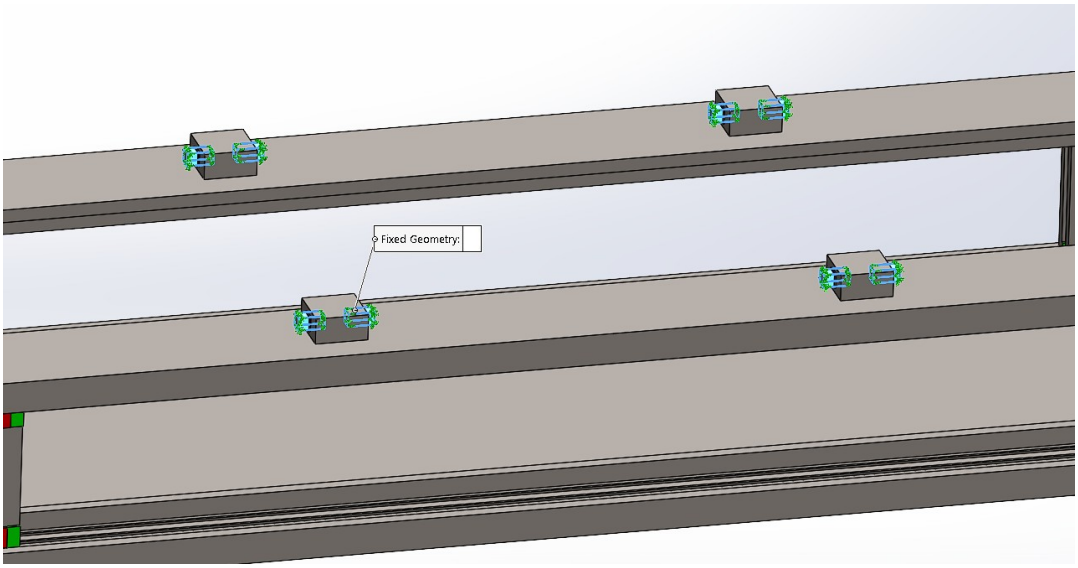

Figure 3.12: Fixed geometry constraint on extensions

As observed in Figure 3.12, the extensions are fully constrained with zero degrees of freedom to emulate attachment to the connection plate. The connections between the mainframe, extendable arms and twist locks previously established in Section 3.1 are directly imported into the simulation pane as bonded contacts. The arms and mainframe utilize bonded contact in the form of stops blocks and the twist locks are bonded to the arms using the locking pins.

Loads: The loads are essentially the forces acting on the spreader frame during operations. The static loads acting on the spreader will be the weight of the container along with the self-weight of the frame. To simulate self-weight, an in-built gravity function is applied perpendicular to the spreader frame in FEA simulation panel. This function is visualized as follows:

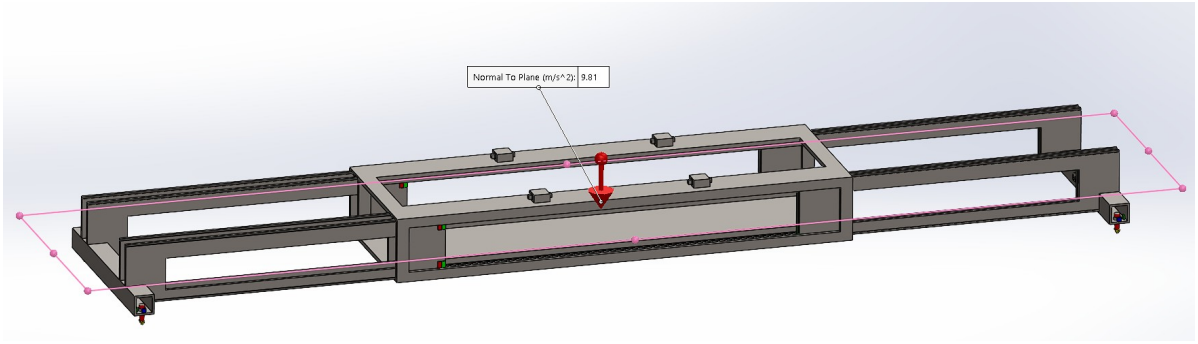

Figure 3.13: Gravity applied on spreader frame

The force generated by the weight of the container will be experienced at the twist locks, since they are the point of contact between the spreader and the container. As per the initial suggestions mentioned in Section 2.2, the weight of the container is taken to be 40,000kgs.

The resultant force is calculated as follows:

$$\text{Container loading force} = \text{Container weight} * \text{Gravitational constant}(9.81 m/s^2)$$

$$= 40000 * 9.81 = 392400N$$

$$\text{On each twist lock, } \textbf{Container loading force } = 343350/4 = 98100N$$

In addition to static load of the container, it is also important to account for the dynamic loads acting on the spreader during operations. These loads are experienced in the form of inertial forces acting on the spreader during transportation. The most significant inertial force is experienced during hoisting a container from the ground. The spreader will be subjected to the dynamic effect of transferring the container load from the ground onto the frame. This force is calculated according to section 4.2 (loads), subsection 4.2.2 (regular loads) from NEN EN 13001-2: Crane safety - General design - Part 2: Load actions [23]. This is the reference standard for load calculations as per the primary standard for container spreaders (NEN EN 15056), mentioned previously in the product requirements.

$$\text{Hoisting inertial force} = \phi * \text{Container loading force}$$

where,
ϕ = dynamic hoisting factor, assumed 1.25 according to Annex A, NEN 15056,
when load combination of hoisting+wind load
Therefore, the hoisting inertial force is calculated as follows:

$$\text{Hoisting inertial force} = 1.25 * 40000 * 9.81 = 490500N$$

$$\text{On each twist lock, } \textbf{Hoisting inertial force} = 122,625N$$

These forces are applied on each twist lock in SolidWorks simulation panel as follows:

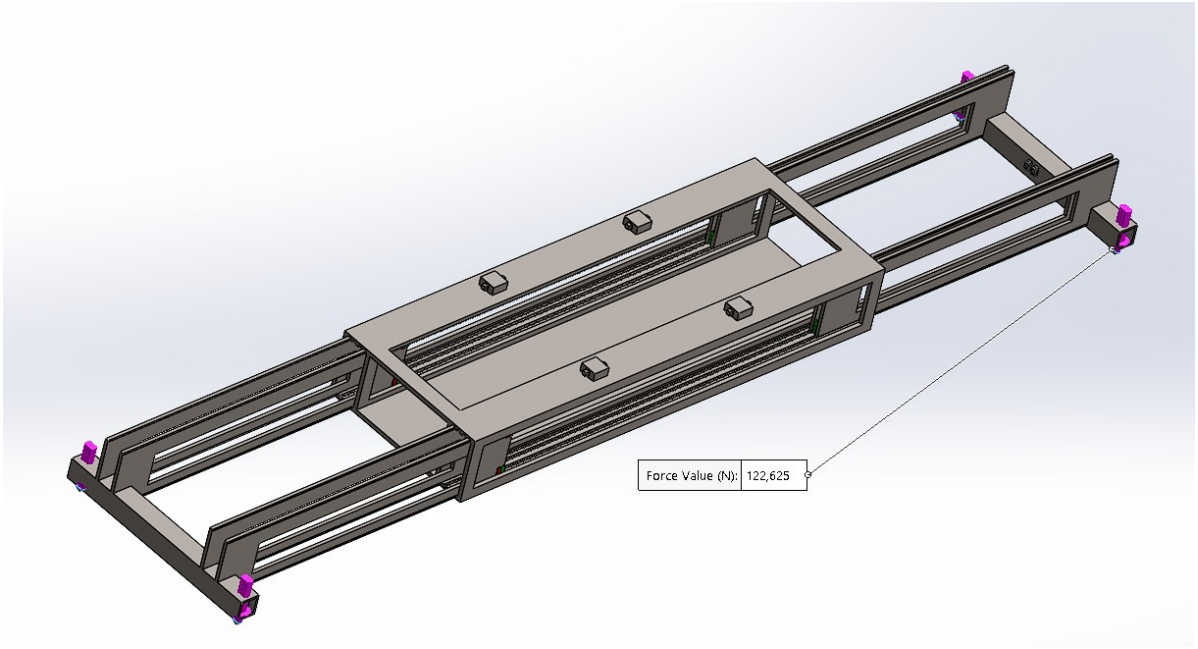

Figure 3.14: Hoisting inertial force acting on spreader frame

As per the product requirements defined in Section 2.2, the spreader should be capable of withstanding all environmental challenges at the terminals during operations. Since container terminals are usually situated in coastal areas, they experience significant winds coming from the sea. Therefore, calculating the in-service wind forces acting on container handling equipment is crucial to verify integrity during operations. These forces are also calculated in a standardized manner, specifically according to NEN EN 13001-2, specifically using the formulas from section 4.2 (loads), subsection 4.2.3 (ocassional loads) [23]. The equation provided for calculating in-service wind load is as follows:

$$F = 0.5 \cdot C_a \cdot \rho \cdot A \cdot v^2$$

where,

F is the wind force
C_a is the aerodynamic co-efficient, assumed to be 2.4 for complex geometries
ρ is the air density, approximately 1.225 kg/m^3 at sea level
A is the projection area, calculated via SolidWorks measurement fucntion
v is the wind speed, taken to be 28 (m/s) for heavy winds scenario

The wind forces could potentially act on the spreader frame in multiple directions simultaneously and therefore it is essential to account for both transverse and longitudinal wind forces. The transverse forces act perpendicular to the chosen spreader frame geometry whereas the longitudinal forces act along the plane of the geometry. The values for these forces are calculated as follows:

Transverse wind force $= 0.5 * 2.4 * 1.225 * 4.34 * 28^2 = 5002N$

Longitudinal wind force $= 0.5 * 2.4 * 1.225 * 0.73 * 28^2 = 842N$

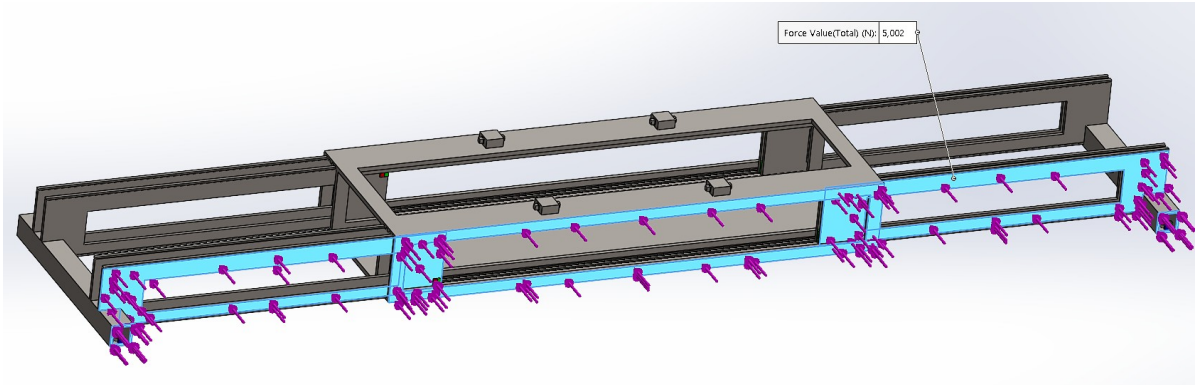

Figure 3.15: Wind force in transverse direction

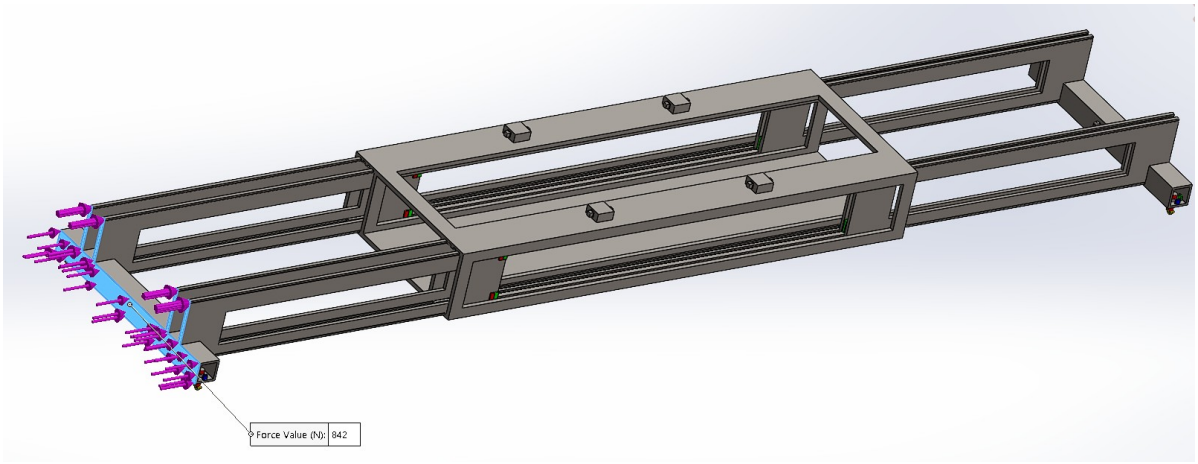

Figure 3.16: Wind force in longitudinal direction

The spreader frame also has to account for the torque generated during rotation of twist locks. This torque is generated at the connecting shaft of the twist lock by the chosen actuation mechanism. The twist lock designed previously in Section 3.1 weighs 6 kgs, as per Solidworks mass evaluation function. Therefore, a suitable torque value for a successful rotation is calculated [24]. The torque is formulated as follows:

$$\text{Torque} = \text{applied force} * \text{Radius of connecting shaft (35 mm)}$$

$$\text{Applied force} = \text{Weight of twist lock} * g = 6 * 9.81 = 58.86N$$

$$\text{Torque} = 58.86 * 0.035 = 2.06Nm$$

The values of torque are significantly lower and will likely not affect the spreader frame during operations. Moreover, the rotation of twist locks only happens when the spreader is suspended above the container without physical contact. Hence, the effect of torque on the spreader frame can be ignored during the analysis.

Element selection: The spreader frame comprises of components made up of various elements, such as beams, shells or solid elements. It is essential to define each component according to their particular element type during FEA to accurately represent behavior during operations. However, since the design of spreader frame is custom and does not use standardized beams/shells, each component is modeled as a solid body to maintain simplicity during analysis.

3.2.2. Analysis

This phase of FEA deals with setting up a test case for simulating the behavior of spreader frame in it's operational environment. The test comprises of a combination of different loads, constraints and boundary conditions to emulate real-world operational conditions of the spreader. The most significant test case is one which imposes the maximum possible stress on the spreader and will thoroughly test the structural integrity during operations. On observing the testing parameters described in Section 3.2.1, it is devised that the scenario exerting the maximum stress on the spreader frame is hoisting a container from the ground during heavy winds. The load combination for this case can be observed as follows:

Test case	Explanation	Load combinations
Hoisting case	Spreader lifting a container from the ground during a storm	Self weight of spreader + Hoisting inertial force + Wind forces both directions

Table 3.3: Test case for Finite Element Analysis (FEA)

This test case will be analyzed using an in-built direct solver offered by SolidWorks simulation to generate results. There are two choices for the solver, namely a linear or a non-linear solver. A linear solver assumes a linear relation between applied loads and occurring displacements whereas a non-linear solver assumes a non-linear relation. This impacts the nature of the stiffness matrix of the assembly that is being analyzed. Usually, an initial linear analysis is conducted to observe the behaviour of the assembly and decide whether to switch over to a non-linear model. This decision is based on the following conditions which could cause non-linear behaviour:

Material behaviour: The chosen material should comply to Hooke's law, which states the relation between the stress and the strain for the material is linear. This is observed until the observed stress remains under the yield strength of the material,i.e., no plastic deformation. If the observed stress value is beyond the yield strength, the material enters the plastic range and exhibits non-linear behaviour.
Direction of force: A linear analysis assumes constant direction of applied force implying that it will not change direction over time due to deformation.
Direction of contact: A linear analysis assumes fixed contact between components and does not account for change over time. Since the extendable are in solid contact with the mainframe via stop blocks and the twist locks are held in position using locking pins, the assembly will not have moving parts when loads are applied.
Minor deformations: The observed deformation due to loads on the assembly should be minimal enough to ignore the change in stiffness of the structure caused by large deformations. Moreover, this also ensures that the change in direction of force is negligible enough to assume linearity. A general rule of thumb states that the deformation should be less than 1/20 th of the length of the longest structure in the assembly [25].

The test case for evaluating the structural integrity of spreader frame is now fully defined. The chosen load combinations are applied in the simulation panel and the solver is activated to generate the required results.

3.2.3. Post-processing

The post-processing stage is where generated results from the simulated test case are visualized and evaluated. The evaluation of FEA is conducted by comparing the observed physical quantities from the simulation to their acceptable limits declared in NEN EN 13001-3-1: Cranes - General Design - Part 3-1: Limit States and proof competence of steel structure [26]. This is the reference standard for verifying structural competence as per NEN EN 15056. Following are the required physical quantities required for verifying competence and their observed values:

1. Von-mises stress (σ_s): This is the stress value used to predict whether a structure will yield/fracture due to axial loading. According to section 5 (proof of static strength) subsection 5.3.1 (execution of static strength) in NEN EN 13001-3, this value should always be less than the calculated limit design stress of the structure (f_R). The limit design stress is calculated as follows:

$$f_r = \frac{f_y}{\gamma}$$

where,
f_y= yield strength of the material chosen for the frame (620 MPa for spreader frame as per Table 3.1)
γ= specific resistance factor, taken as 0.95 for rolled materials such as stainless steel alloys.

$$f_r = \frac{620}{0.95} = 652.63MPa$$

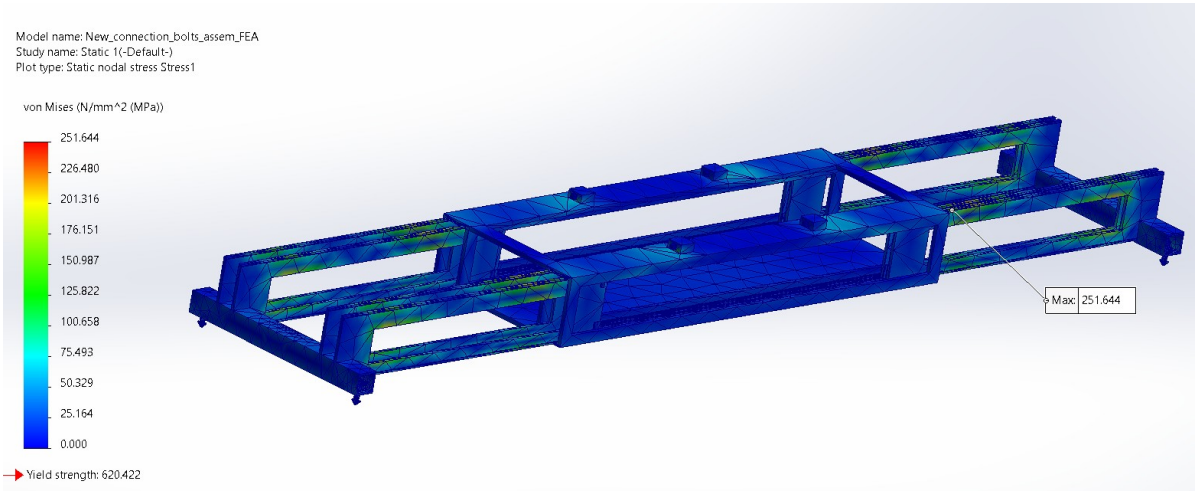

Figure 3.17: FEA Hoisting case: Von mises stress

As observed from Figure 3.17, the maximum value of von-mises stress is observed to be $\sigma_s = 251MPa$ which is well below the limit design stress of the structure, hereby proving competence for the chosen application.

2. Factor of safety (FOS): This value evaluates the load bearing capacity of a structure beyond its applied force. According to section 6 (verification of safety requirements) of NEN EN 15056, a proof load test is conducted with 1.5 times the rated capacity, implying that the spreader frame should be able to handle 1.5 its maximum working load without yielding. This value is calculated as follows:

$$\text{FOS} = \frac{\text{Yield strength of material}}{\text{Von mises stress}} \geq 1.5$$

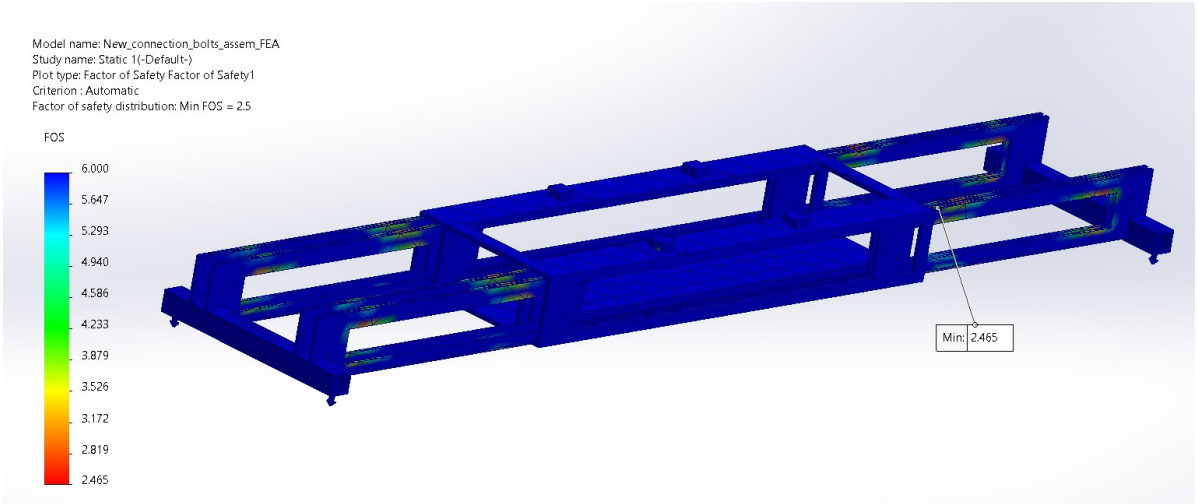

Figure 3.18: FEA Hoisting case: Factor of safety (FOS)

As observed from Figure 3.18, the observed FOS value is 2.465 meaning that the spreader is capable of handling up to 2.4 times it's rated capacity. Therefore, the spreader frame has passed the proof loading test.

3. Strain (ϵ): This value is utilized to evaluate the elastic/plastic deformation of a structure under loading. To prevent the structure from permanent deformation, the value of strain must remain below it's elastic range/limit [27]. This range is calculated as follows:

$$\epsilon < \frac{\text{Max. normal stress}}{\text{Young's modulus of material (E)}}$$

where E=210 GPa from Table 3.1 and the maximum normal stress value acting on the spreader frame is observed to be 361 MPa from Figure 3.19.

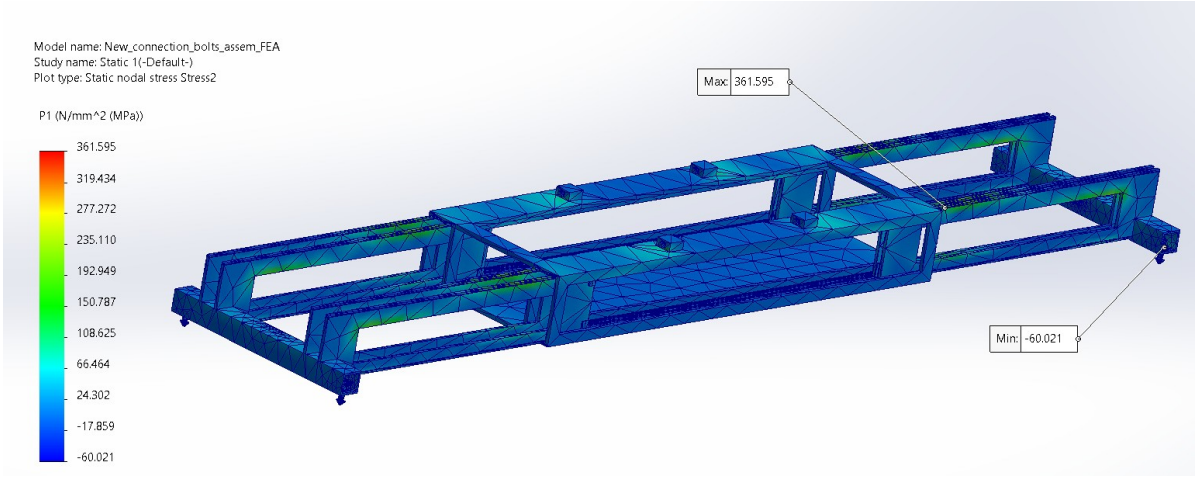

Figure 3.19: FEA Hoisting case: Principle stresses

This provides a calculated allowable limit of :

$$\epsilon < \frac{361 \text{ MPa}}{210 \text{ GPa}} = 1.71e-03$$

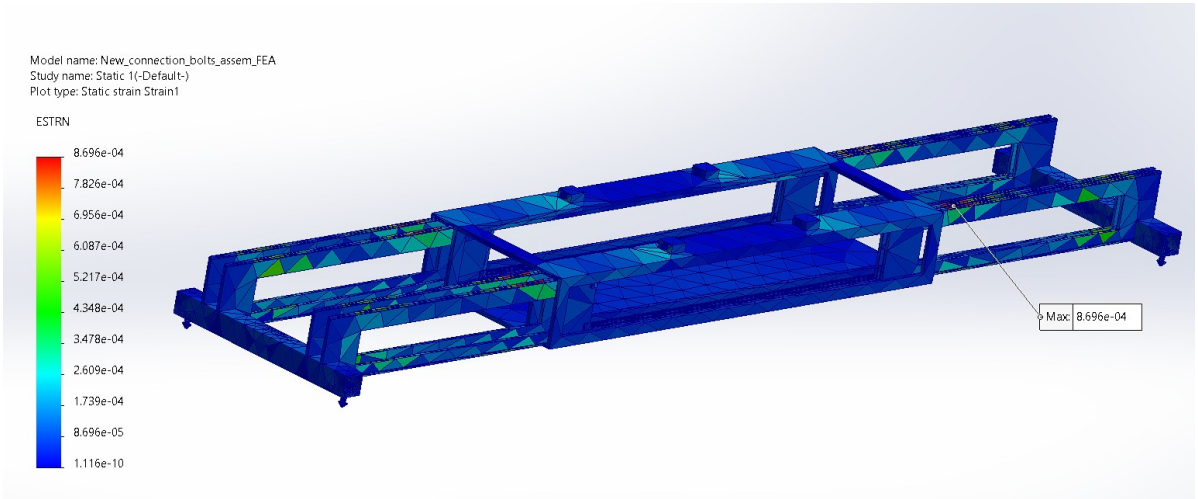

Figure 3.20: FEA Hoisting case: Equivalent strain

According to Figure 3.20, the maximum equivalent strain was observed to be $\epsilon = 8.69e-04$ which is below the allowable limit proving that the spreader frame remained it's elastic zone and did not exhibit plastic behaviour.

4. Shear stress (τ): This value is the stress generated due to shearing forces acting on the spreader during operations. According to section 8 (proof of elastic stability) subsection 8.3.1 (Limit design stress with respect to shear stress) in NEN EN 13001-3, the limit for this value is calculated as follows:

$$\tau = \frac{(\text{Material yield strength} * \text{reduction factor (=1)})}{\sqrt{3} * (\text{General resistance factor} \gamma_m = 1.1)}$$

$$\tau = \frac{(620 * 1)}{\sqrt{3} * 1.1} = 325.41 MPa$$

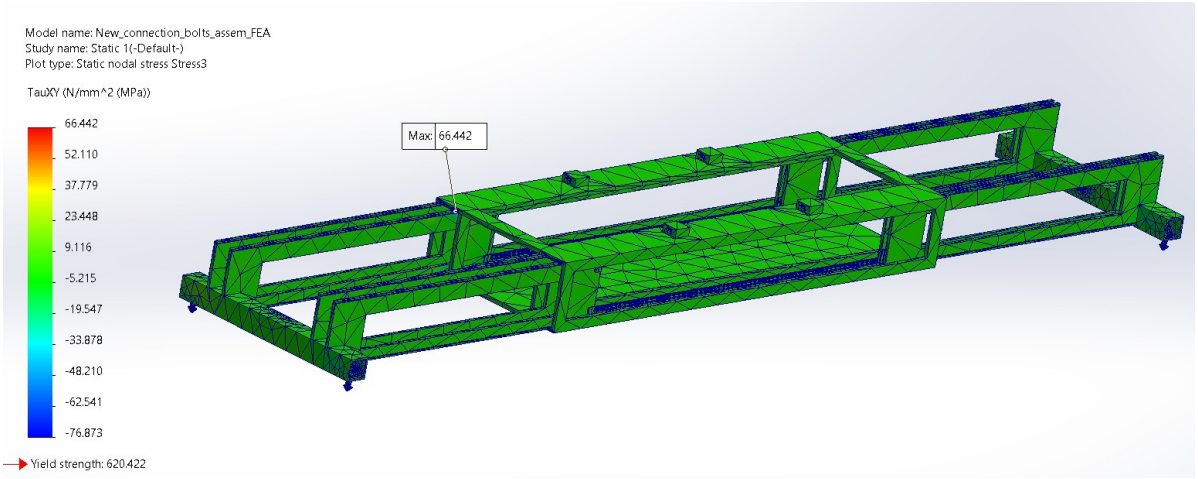

Figure 3.21: FEA Hoisting case: Shear stress

The observed value of shear stress is $\tau = 66.4 Mpa$ which is well below the calculated limiting value. Therefore, the frame is within the allowable shear stress limits as per the design safety standard.

5. Deflection (δ): This value evaluates the maximum lateral deformation experienced by a structure during axial loading. According to section 8 (proof of elastic stability), Table 13 (acceptable bow imperfections for various cross sections) in NEN EN 13001-3, this value should not exceed certain limits for the structure to remain competent. For solid cross-sections such as the one of the spreader frame, this limit is declared as follows:

$$\delta \leq \frac{\text{Total span length of structure}}{200} = \frac{12450}{400} = 62.25 mm$$

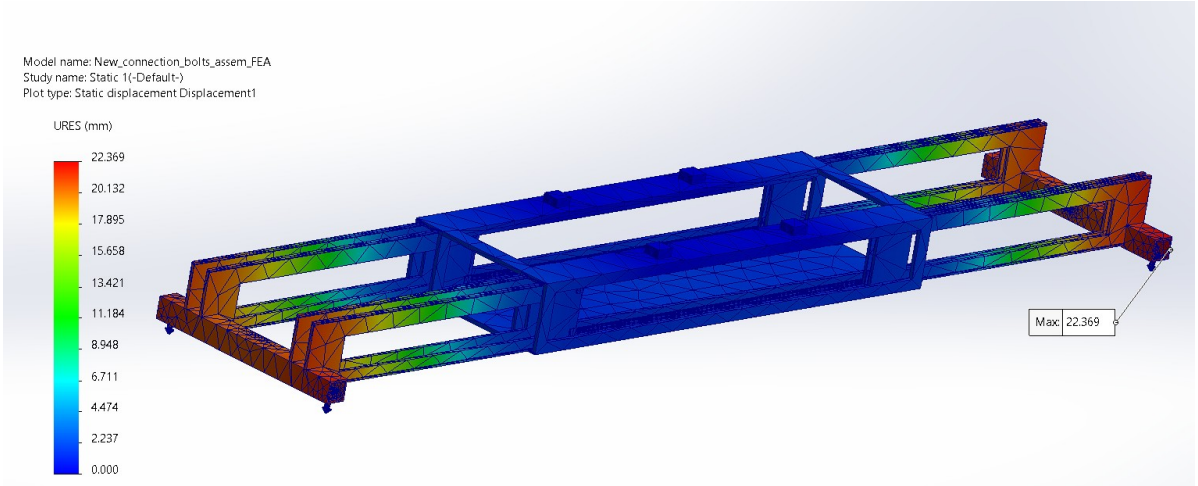

Figure 3.22: FEA Hoisting case: Maximum displacement

From Figure 3.22, the value of deflection is observed to be $\delta = 22.3 mm$ which is well below the declared limit. Therefore, the frame is competent in terms of it's lateral deflection limits.

6. Buckling (BLF): Buckling is defined as a sudden deformation/fracture of a structure under loading. This is a dangerous situation and can lead to significant damage and risk of accidents. Therefore, it is necessary to know the critical buckling load applicable to a structure. The stability of the structure is confirmed if the Buckling load factor(BLF),i.e., ratio of the critical buckling load to the applied axial load satisfies the following criteria:

$$\text{BLF} = \frac{\text{Critical buckling load}}{\text{Applied axial load}} > 1$$

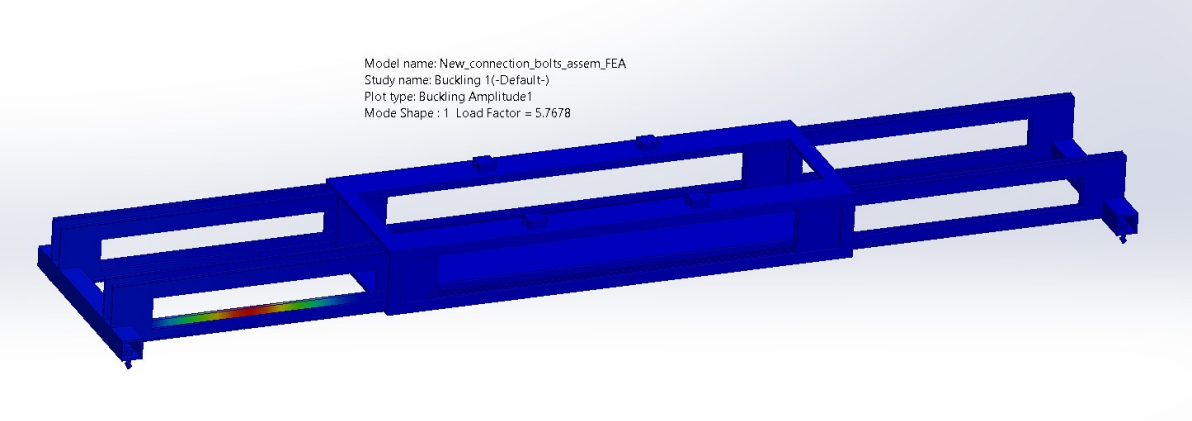

Figure 3.23: FEA Hoisting case: Buckling load factor (BLF)

As observed from Figure 3.23, the load factor value is 5.7, indicating that the spreader frame can handle up to 5.7 times it's applied load before experiencing buckling. Hence, the frame is feasible for the chosen application. All relevant physical quantities have now been identified and evaluated for verifying structural competance. These evaluations can be summarized as follows:

Quantity	Value	Criteria as per NEN 13001-3-1	Competence
Von mises stress	251.6 MPa	Below yield strength value of 652.63 MPa (Table 3.1)	Yes
Factor of safety	2.465	greater than 1.5	Yes
Principle stresses	Max: 361 MPa Min: -60 MPa	-	-
Shear stress	66.4	Less than $\tau < \frac{620}{\sqrt{3}*2.465} = 325.41MPa$	Yes
Equivalent strain	8.69 e-04	Less than $\epsilon < \frac{361MPa}{210GPa} = 1.71e-03$	Yes
Maximum displacement	22.3 mm	Less than 62.25 mm	Yes
Buckling load factor	5.76	Greater than 1	Yes

Table 3.4: FEA: summary of structural integrity verification

3.3. Findings from FEA

The observed von-mises stress and strain values remained well below the critical limit of the chosen material. Moreover, the observed displacement of 22.3 mm is less than 1/20th of the maximum of structural length ($\frac{12450}{20} = 622.5mm$). Therefore, proceeding to a non-linear analysis is not necessary as the assembly satisfies all the conditions defined in Section 3.2.2. The iterative cycle to verify the structural integrity of the spreader frame is now complete. The spreader frame has fulfilled all the NEN 13001-3-1 safety reference standards as per NEN-EN 15056. The frame remained within allowable limits and did not yield/buckle in its test scenario and therefore can be considered feasible for operation. It is now feasible to install all the required actuators and sensors onto the spreader frame and analyze their functioning.

4. Iterative cycle for operational feasibility

This cycle of iterations involves development of suitable technology required to enable automated operations of the spreader. Firstly, all the components required for feasible operations along with their expected power consumptions are defined in Section 4.1 and installed onto the spreader frame. Secondly, an appropriate control algorithm is created, tested and evaluated in Section 4.2. Finally, a product requirement verification for both iterative cycles is conducted in Section 4.3 .

4.1. Required components and power consumption

The spreader handling process requires a variety of different components to enable operations. These components can be classified as the actuators and sensors necessary for smooth and reliable functioning. The necessary components are chosen considering the limitations observed in the current apparatus of components in Section 1.2 along with the product requirements and initial concept suggestions mentioned in Section 2.2. All actuators and sensors chosen for operations can be specified for feasible Ingress Protection (IP) rating. This is a two digit rating which grades the resistance of an electrical component against exposure to solids and moisture. The first numeral dictates protection against solid contaminants and the second numeral against liquid contaminants. Considering the harsh environmental conditions the spreader will potentially experience and the open frame design which exposes internal components, it is feasible to choose an IP rating greater than 65, where ”6” indicates zero dust ingress allowance and ”5” indicates protection against water jets [28]. The locking pin actuators and quick release actuators have been ignored for the analysis since they are not expected to consume much power due to minimal travel distances and size.

4.1.1. Actuator for arm extension:

Since the spreader frame is following a fixed width variable length design, extendable arms are utilized to provide the extra length for FEU container transport. Therefore, suitable linear actuators are necessary to extend the arms to their required position. This is mainly achieved via utilizing either hydraulic or electric actuators. Hydraulic actuators are the current industry practice primarily due to their robust nature and high load carrying capacities. However, they require significant maintenance and have also raised environmental concerns due to fluid leakage possibilities. Hence, it is preferable to consider heavy-duty electric actuators since they offer the highest precision and control integration capabilities [29]. On investigating all available electric actuators, an appropriate option for arm extension was deduced to be the use of telescopic ball-screw actuators.

Working principle: These actuators are ideal for high-load moderate speed applications like extension of spreader arms. They consist of a rotating screw paired with a ball nut that converts rotary motion provided by a motor into smooth linear motion. Multiple telescopic tubes are utilized to enable longer extension lengths while maintaining compact initial size. The load is attached to the outermost tube and aligned with other tubes using in-built linear guides. This actuator also consists of an anti-rotary nut that prevents reverse motion [30].

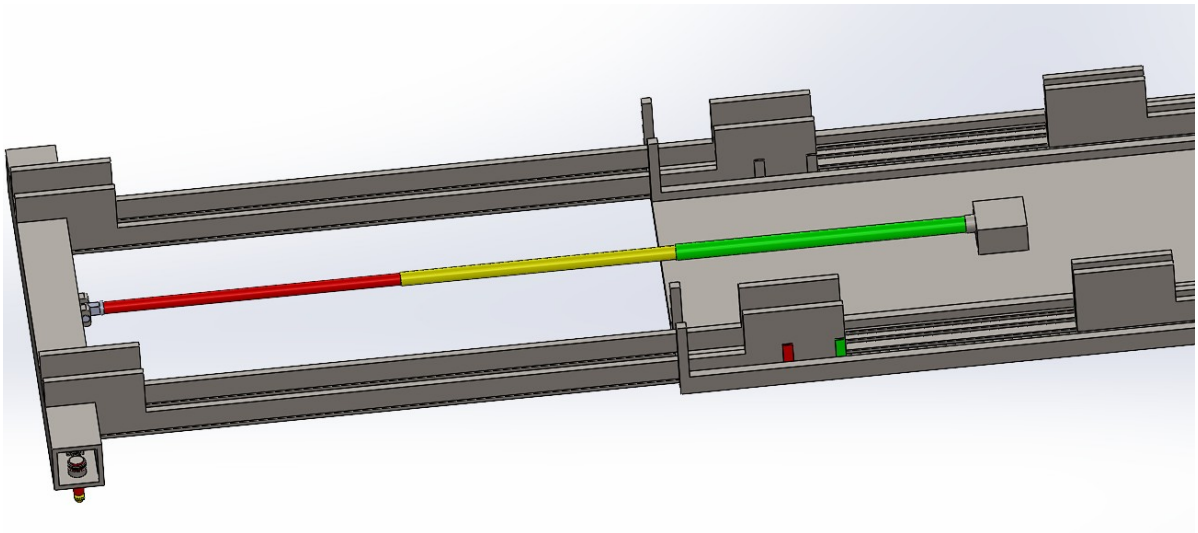

Figure 4.1: Linear telescopic electric actuator for arm extension

Area of application: As observed in Figure 4.1, a three-stage telescopic actuator is installed on the bottom base plate of the mainframe with the outermost tube connected to the frame of the extendable arms. The maximum telescopic length of the actuator is according to the extra length required to align with FEU container castings whereas a fully-contracted length is designated for TEU container transport.

4.1.2. Actuator for twist lock rotation

The spreader utilizes twist locks to lock/unlock onto a container for transportation. Currently, a drive linkage connected to a centralized actuating mechanism is utilized to rotate the twist locks. This leads to more moving parts increasing the number of failure points in the assembly and restricts individual control over each corner. To solve this issue, four independent actuators can be installed at each corner of the spreader. There are multiple options to choose from for these actuators, namely servo motors, stepper motors and Direct Current (DC) motors. DC motors offer the most robust functions with minimum control possibilities and are usually used for high revving operations. Servo motors offer the highest precision over rotation but require extensive tuning and maintenance. Stepper motors are an ideal middle ground offering decent precision and control over rotation [31].

Working principle: These motors convert signals into a defined rotational position in the form of incremental steps to allow precise motion. The electric signals will be provided by the control system programmed to generate appropriate signals for pulses, speed and direction of motion. Moreover, these motors are comprised of a feedback loop provision to provide additional sensor output back to the control system for extra precision. These motors are a cost-effective option and offer reasonable torque at moderate speed [32].

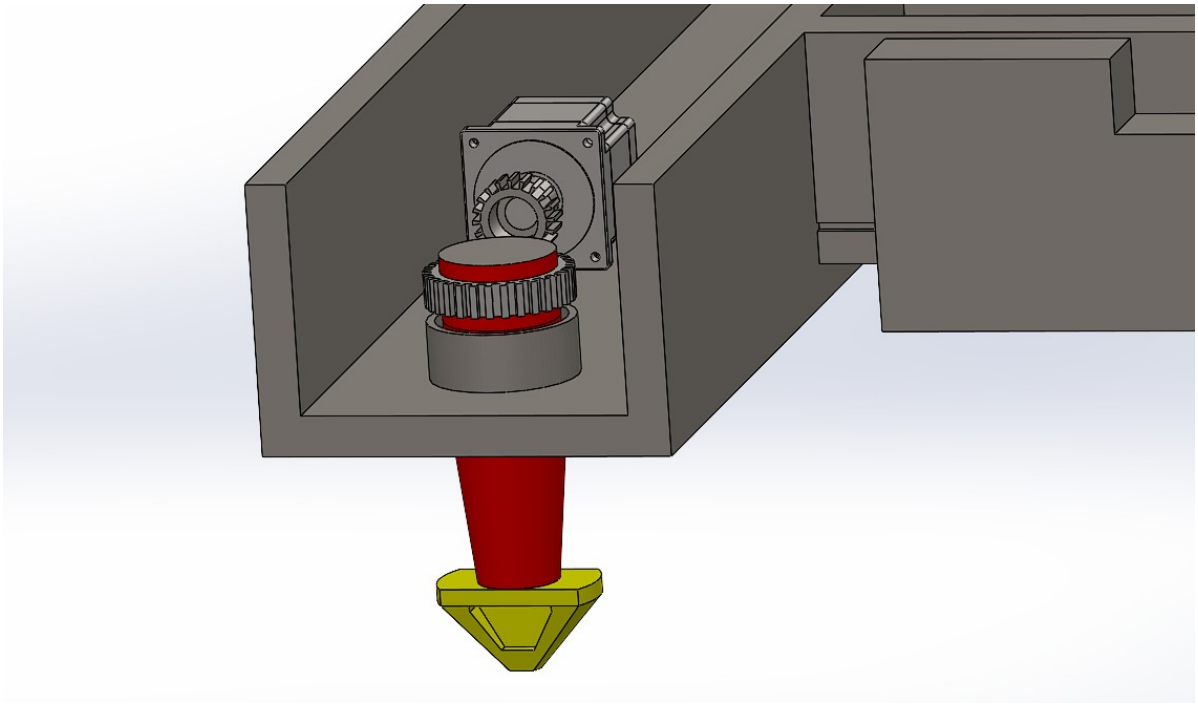

Figure 4.2: Sectional view: Stepper motor installed for rotation of twist locks

Area of application: They are installed inside the spreader arm frame and connected to the shaft of the twist locks via a suitable gear assembly. As observed in Figure 4.2, the stepper motor and the connecting shaft of the twist locks are connected via a bevel gear mechanism. The gear is installed onto the connecting shaft of twist locks and the pinion is attached to the rotating shaft of the stepper motor. This reduces the number of moving parts for rotation and consequently transfers the power required for rotation of twist locks from the stepper motor to the connecting shaft.

4.1.3. Sensor for identifying arm position

Identifying the position of extendable arms is vital to ensure appropriate alignment of the spreader with respect to a container for transport. This is achieved by utilizing a position sensor which measures the displacement of an object compared to a certain reference point [33]. The arm extension actuator previously defined in Section 4.1.1 can be equipped with an in-built linear encoder that identifies the position of the arm at all times which can be used by the control system to confirm arm position.

4.1.4. Sensor for identifying spreader-container engagement

Once the spreader is aligned with the corner castings of a container, it is lowered until the twist locks are immersed sufficiently into the castings to begin rotation. Therefore, a sensor is required to confirm adequate lowering of the spreader to prevent physical collision between the spreader and container. Currently, a landing pin connected to a limit switch is installed below the spreader frame at each corner for detecting contact with container. Once the pin is pushed back by the container to it's calibrated value, the limit switch gets activated and alerts the operator to stop lowering. This pin always required physical contact for a successful detection and therefore will require frequent maintenance and replacements. Moreover, if a corner casting gets damaged during transport, landing pin accuracy could be affected due to surface irregularities. Furthermore, the limit switch cannot provide continuous monitoring of the distance between the spreader and container. Hence, a no-contact detection sensor which can constantly detect target distance is deemed to be an appropriate alternative. For this particular application, an inductive proximity sensor is suitable.

Working principle: It detects a nearby metallic object of interest without physical contact. It operates on the principle of eddy current generation where the sensor consists of a magnetic coil in which a current is induced due to arrival of a metallic object such as a container. The sensor can constantly observing the changes in oscillations by the induced current created by the target container. When the container comes within a specified range, the generated induced current value can be calibrated as a peak to prompt the production of an output signal that is used by the control system to stop lowering of the spreader. It is ideal for the short range application of identifying proximity between the spreader and container and requires minimal maintenance only for calibration once a year since it avoids physical contact. Moreover, it is not affected by external factors like light, temperature and humidity [34].

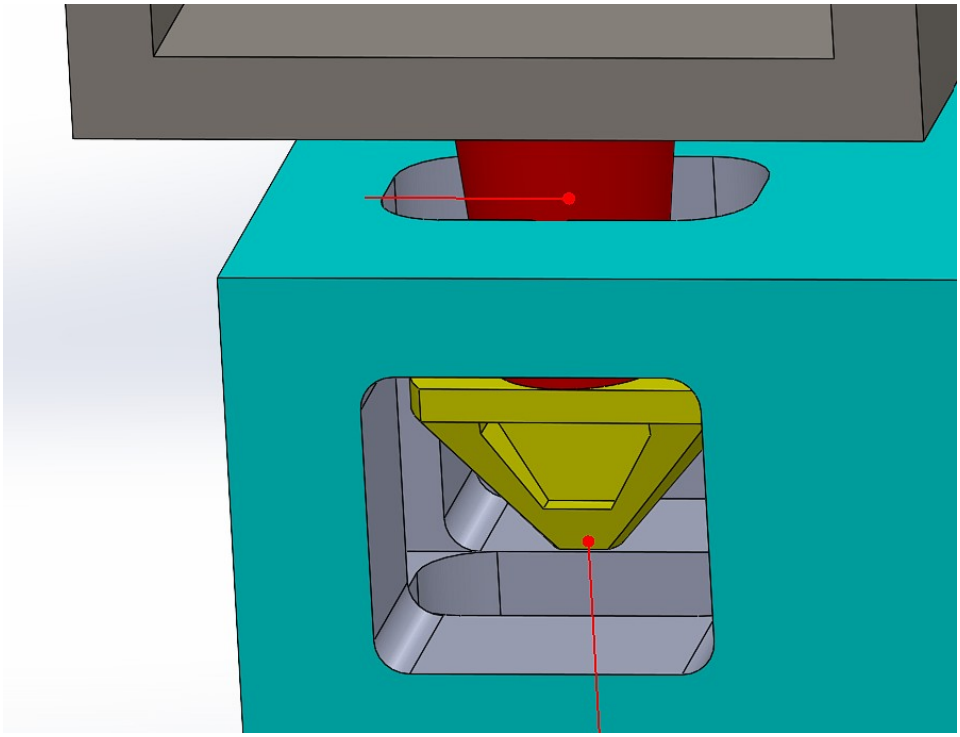

Figure 4.3: Inductive proximity sensor for container detection

Area of application: For accurate identification of proximity, it is feasible to install a sensor at each twist lock of the spreader. The control system can be programmed to confirm proximity only after feedback is received from all four sensors. This prevents partial immersion of twist locks in either corners and ensures sufficient clearance to begin rotation. Furthermore, to prevent external interference and maintain minimal proximity range, the sensors should be ideally enclosed at the very end tip of the twist locks. A redundant sensor can also be installed in the connecting shaft to prevent extra/insufficient lowering caused by accidental tilting of the spreader or container.

4.1.5. Sensor for identifying twist lock orientation

It is necessary to identify the position of the twist locks during operations to ensure safe lifting and lowering of the spreader from containers. This is a vital step during the handling process since insufficient locking/unlocking can potentially result in the spreader dropping the container causing accidents and injuries in the terminal. A combination of hall-effect sensors are observed to be the ideal choice.

Working principle: These sensors utilize the principles of hall effect in which a potential difference is observed when a moving magnetic field is introduced in a flowing current. The moving magnetic field generates a range of potential differences which can be calibrated according to the required orientations for complete locking/unlocking. This sensor allows continuous measurement of orientation and therefore can be used to identify partial locking/unlocking as well. These sensors are robust as they do not require physical contact for identifying orientation and can be appropriately shielded to avoid potential magnetic interference [35].

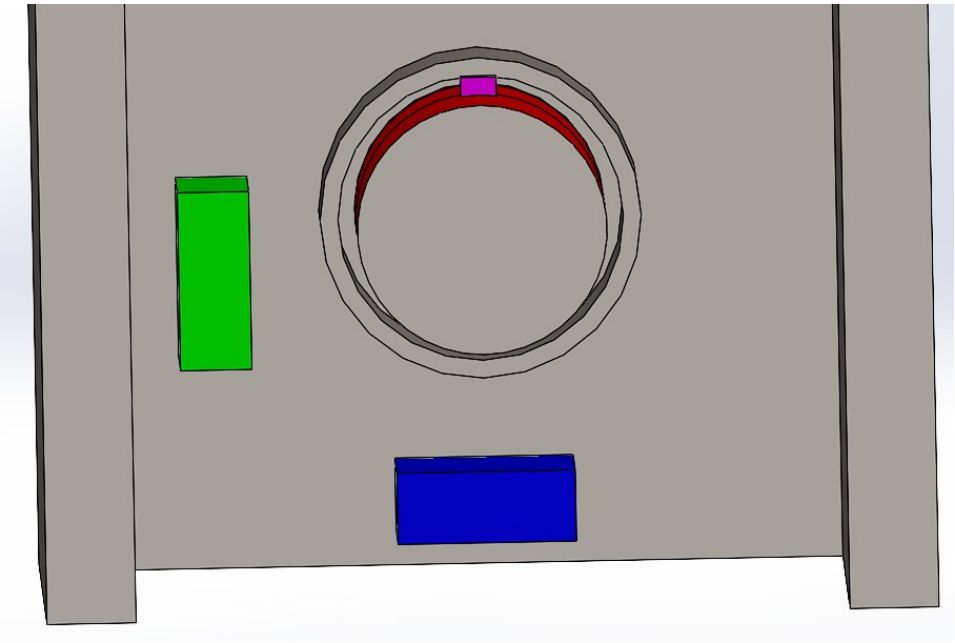

Figure 4.4: Magnet (pink) attached to connecting shaft with two hall sensors (green for locking blue for unlocking)

Area of application: To ensure each twist lock has appropriately locked/unlocked onto a container, it is preferable to install a pair of hall-effect sensors are each corner of the spreader. The moving magnet can be attached to the connecting shaft of the twist locks and the sensors can be installed at a suitable location in the frame of extendable arms. When the shaft rotates by 90 degrees to lock, the magnet faces the first sensor and this generates feedback for confirmation of locking by the control system. When the shaft rotates further to 180 degrees to unlock from the container, the magnet faces the second sensor calibrated to provide feedback for unlocking. At the end of one operating cycle, the shaft is rotated to a full 360 degrees to reset the position of the magnet and sensor values.

4.1.6. Power consumption of spreader

The necessary sensors and actuators have been successfully defined for spreader operations. Since the spreader is expected to possess an internal supply of power as per the product requirements in Section 2.1, it is necessary to evaluate the power consumption of these components to evaluate the battery specifications and required allocation of space in the frame. The consumption figures for each component are calculated based on necessary assumptions as follows:

Ball-screw actuator: The mass of each extendable arm is 2700 kgs as per SolidWorks evaluation, and the extension required for FEU lifting spans 3 meters. An average time of 20 seconds for full extension is assumed for calculation:

$$Power = \frac{Work}{time}$$

$Work =$ Force x distance $= 2700 * 9.81 * 3 = 79461J$

$$Power = \frac{79461}{20} = 3973W$$

For 2 extension actuators, Power = $3973 * 2 = 7946W$

Stepper motors: The torque required for rotation of twist locks is 2 Nm as per the calculations conducted in Section 3.2.1. Considering efficiency loss, the required torque is taken to be 4 Nm. A suitable option for achieving this torque is assumed to be a NEMA 34 stepper motor which operates on 48 V direct current at an operating current of 5 A [36]. Hence the power required is:

$$Power = V * I = 48 * 5 = 240W$$

For 4 stepper motors, Power=$240 * 4 = 960W$

Proximity sensors: A sample proximity sensor appropriate for detection application is chosen for the calculation. The sensor has a consumption of 10 mA at an average operating voltage of 24 V [37]. Hence, the power consumption is calculated as :

$$Power = V * I = 10/1000 * 24 = 0.24W$$

For 4 proximity sensors, Power $= 0.96W$.

Hall-effect sensors: A sample sensor data sheet is referred for calculations. It states that the sensor requires 25mA of continuous current at a peak voltage supply of 24 V [38], therefore the power consumption is calculated as follows:

$$Power = 25/1000 * 24 = 0.6W$$

For 8 sensors, Power $= 8 * 0.6 = 4.8W$

The total power consumption of the spreader is estimated to be about 9 kW at a maximum operating voltage of 48 V. Hence, the discharge current required by the battery is 9000/48 = 187 A. On analyzing currently available options for electric power supply, lithium iron phosphate (LiFePO4) battery cells are considered to be the most feasible solution. These cells can provide high efficiency figures for an extended period of time in a limited structural weight and compact size [39]. The specifications of these cells are listed as follows [40]:

EVE LiFePO4 cells
Capacity = 304 Ah
Discharge current = 304 A
Voltage= 3.2 V
Weight = 5.5 kgs
Dimensions= L 173.5 x W 72.0 x H 208.8 mm

Table 4.1: Datasheet of chosen battery cell for spreader

To achieve the required maximum output of 48 V, it is necessary to create a pack of 15 such cells connected in series. This pack is configured by stacking 3 rows of 5 cells in series. Since the sensors require a lower operating voltage, a DC buck converter can be utilized to step-down the supplied 48 Volts to 24 V [41]. The mainframe of the spreader is capable of fitting 16 such packs in the following configuration:

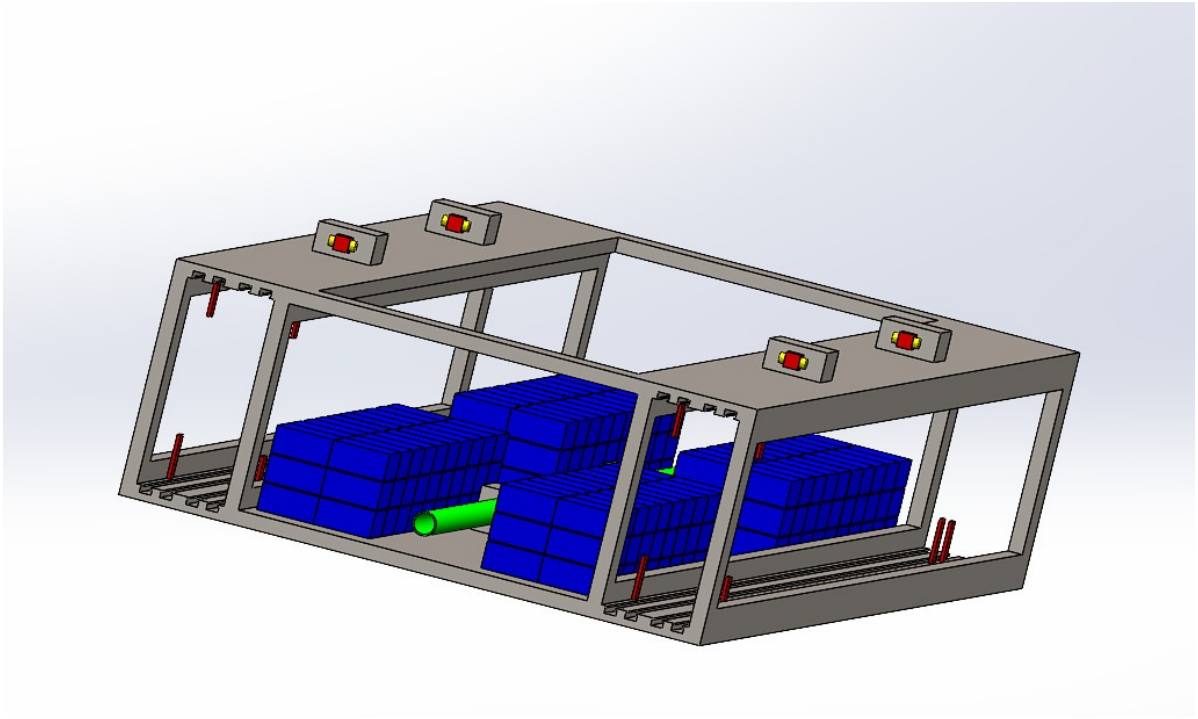

Figure 4.5: Four battery packs at each corner of the mainframe

The total power available by this battery configuration is calculated as follows:

$$\text{Power output of each pack} = 304 * 48 = 14592W$$

Power output of 16 packs= 233,472W = 233 kW

Considering an average system efficiency of 80 percent accounting for losses due to batteries, actuators, sensors and wiring, the estimated operating time by the spreader are calculated as follows:

$$\text{No. of operating hours} = \frac{\text{Total power output x Efficiency}}{\text{Power consumption}} = \frac{233 * 0.8}{9} = 20 \text{ hours}$$

This battery configuration allows the spreader to operate independently for roughly 20 hours. Whenever the battery of the spreader is about to be drained, it can be replaced quickly with fully charged packs by lowering the spreader on the ground and lifting the batteries from the top using a small crane or lifting arm. All the required components for enabling automated operation of spreaders are now defined. These components require appropriate control integration for reliable functioning of the spreader.

4.2. Control algorithm for automated operations

The components required for automated operations defined in Section 4.1 need an appropriate integration method to enable independent locking/unlocking of the spreader. On observing the current operating procedure of spreader handling, it is observed that each component (actuator/sensor) functions in discrete phases based on which particular stage of the handling process the spreader is executing. Once the component executes its function in that stage, the next component is activated upon confirmation. Therefore, a **Finite state machine** control algorithm is observed to be the appropriate choice for this particular application. This technique conducts operations in discrete phases/states and allows transitioning from one state to another based on predefined trigger conditions. This algorithm also allows an error state which can halt further operations in case of failure during transitions [42]. To simulate this algorithm, a sample state flow chart is created on MATLAB Simulink where the entire operation of the spreader's twist lock handling is broken down into a finite number of states. Each state has certain pre-defined tasks to be performed and the transition from one state to another is based on the feedback received from the relevant sensors. All sensor readings have pre-defined threshold values and transition only occurs when feedback received from all sensors have satisfied their threshold. Since the focus of this simulation is targeted to understand only the automated twist locking mechanism of spreader, certain assumptions have to be accounted for in the state-chart. The type of container to be lifted is predefined (FEU), therefore, extendable arms are assumed to already be in a fully extended position and the position sensors are not integrated in the state chart. Since the global position of the spreader is not known with respect to the container, the spreader is assumed to be perfectly aligned with its target container and can be lowered directly. Furthermore, the location of the container's destination is not known, hence, the state chart assumes that the spreader always reaches the desired location. Moreover, the height to which the spreader needs to be lifted away is not known, therefore, it is assumed that lifting operations are always successful. Let's understand the state-wise distribution of the spreader handling process along with their transition conditions.

4.2.1. State distribution and transition criteria

The entire process of transporting a container from it's origin to it's destination is broken down into a finite number of states. Each state has designated tasks to be performed by the associated actuator and the transition from one state to another depends on pre-defined criteria.

Idle: This is the default state of the spreader where the system awaits confirmation to begin lowering the spreader. Ideally, this confirmation should arrive once the spreader has located it's target container and positioned itself directly above. However, since the position of spreader is assumed to be directly above the container, a user based switch block (START/STOP) is created to initiate the chart and transition to the next state.

Transition: User changes the switch position from STOP to START.

Lowering: The empty spreader begins lowering onto a target container at it's origin in this state. The actuator for lowering the spreader is initiated and the system observes all the proximity sensor values to verify sufficient engagement between spreader and container.

Transition: Once the state chart recognizes that all proximity sensor readings have accomplished threshold, it initiates a transition to the next state.

Locking: On achieving adequate engagement to container, the system instructs to stop the spreader's lowering actuator and to start the stepper motors for twist lock rotation. While the motors are rotating the locks by 90 degrees, the system observes all the sensor readings from the locking hall-effect sensors to verify orientation of twist locks.

Transition: Once the chart identifies that all locking sensor values are at their threshold, the chart initiates transition to the next state.

Lifting loaded: The steppers motors are deactivated and the locking pins are activated to engage into the twist locks. The actuator for lifting the loaded spreader is also activated in this state. Based on the previously defined assumption that lifting operations are always successful, the chart assumes that the spreader has been lifted and transported above it's desired location and is waiting to be lowered at the container's destination.

Transition: A step block is used as the input parameter which assumes that the loaded spreader always reaches it's destination after a particular amount of time. This confirmation is used to transition to the next state.

Lowering destination: The actuator for lowering the loaded spreader is once again activated in this state. Once the spreader has placed the container on the ground, it is lowered further until the twist locks break contact from the corner castings and are cleared for unlocking from the container. The system uses the proximity sensor readings to confirm this clearance.

Transition: Once all proximity sensors reach their pre-defined threshold again, the chart transitions to the next state.

Unlocking: the lowering actuator is deactivated and the locking pins are instructed to disengage from the locks. The stepper motors are reactivated to rotate 180 degrees for unlocking the spreader from the container. While the motors perform their task, the chart observes the unlocking hall-effect sensor values to verify orientation.

Transition: Once the chart identifies that all unlocking sensor values are at their threshold, the chart initiates transition to the next state.

Lifting unloaded: The steppers motors are deactivated and the actuator for lifting the now empty spreader is activated in this state. Once again, based on the previously defined assumption that lifting operations are always successful, the chart assumes that the spreader has been lifted and cleared from the container.

Transition: Another step block is used as the input parameter which assumes that the empty spreader always clears from the container after a particular amount of time. This confirmation is used to transition to the next state.

Resetting: Once the spreader has cleared away from the container, the lifting actuators are halted and the steppers motors are reactivated to complete a full 360 degree rotation to reset the twist lock orientation and prepare for the next operation. The chart assumes a step block to verify the completion of resetting tasks and uses this block to transition back to the idle state.

Error: This is an emergency state introduced in the state-flow chart. It is connected to all the states which currently depend on sensor feedback for transition. If any of the sensor values fail to meet their pre-defined threshold, the system abruptly transitions into this state and prevents further transitions to the subsequent states. This is an emergency feature that can potentially safe-guard operations and prevent damage or injuries. All states and their transitional criteria have now been successfully defined. The state flow chart can be visualized as follows:

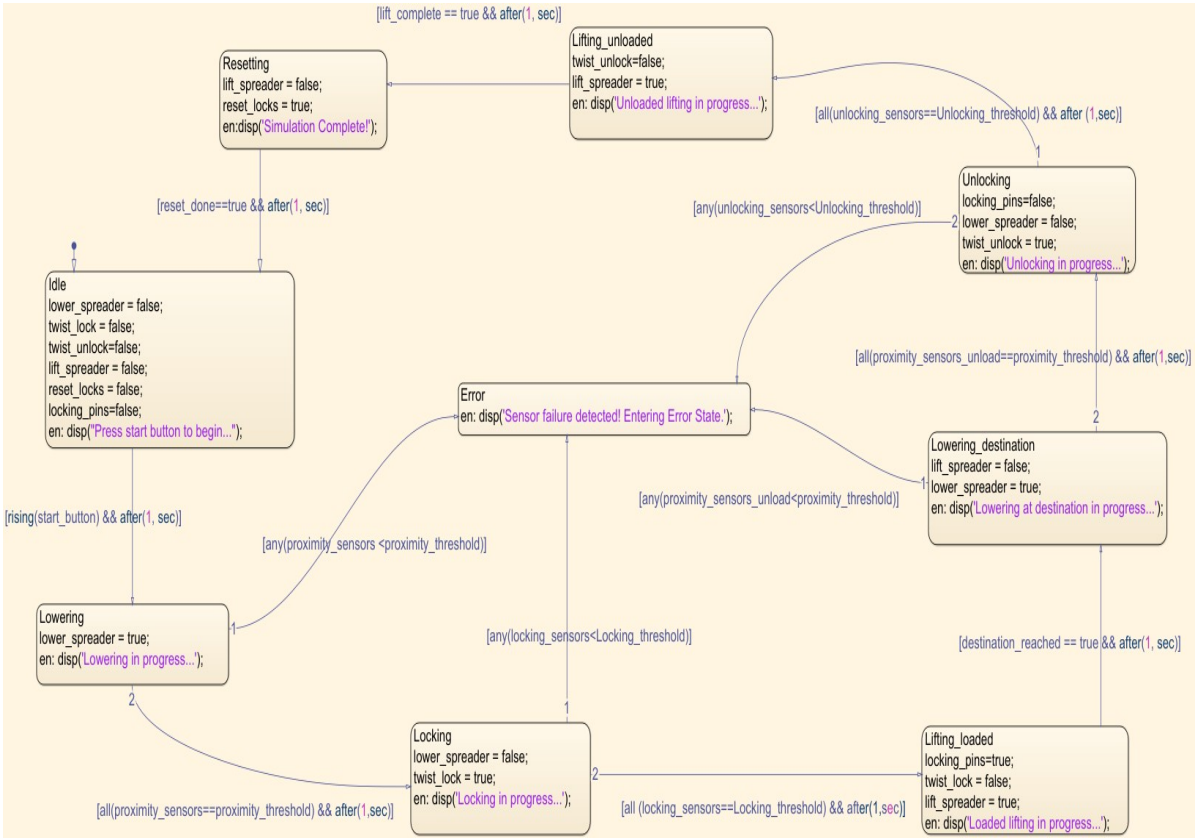

Figure 4.6: State-flow chart on simulink for automated spreader operation

4.2.2. Testing for operational feasibility

The state-flow chart created for automated locking/unlocking operations requires thorough testing for verifying feasibility. Therefore, a test case is setup with appropriate input and output parameters to evaluate the state-chart feasibility. For triggering the transitions in the state flow chart, input data is required for each condition with it's data type, size and initial value. Based on the assumptions defined previously, some transitions are not dependent on sensor feedback and are assumed to be always successful. Therefore, it is feasible to use boolean logic for these transitions, observed as follows:

Input data	Nature	Size	Initial value
start_button	boolean	1	False/STOP
destination_reached	boolean	1	False
lift_complete	boolean	1	False
reset_done	boolean	1	False

Table 4.2: Boolean input data for each transition

The transitions which do depend on sensor feedback require continuous monitoring of signal values by the control system to check whether they have reached their pre-defined threshold. A sample data set is created in the MATLAB workspace for reference. Initially, the data set assumes that all sensor values reach their designated threshold resulting in a successful operation cycle. This data is tabulated as follows:

Sensor input	Nature	Size	Time	Signal values
Proximity_sensors (threshold= 60)	uint16	[1x4]	0 1 2	[0,0,0,0] [30,30,30,30] [60,60,60,60]
Locking_sensors (threshold= 90)	uint16	[1x4]	0 1 2	[0,0,0,0] [45,45,45,45] [90,90,90,90]
Unlocking_sensors (threshold= 180)	uint16	[1x4]	0 1 2	[90,90,90,90] [135,135,135,135] [180,180,180,180]
Proximity_sensors_unload (threshold= 60)	uint16	[1x4]	0 1 2	[50,50,50,50] [55,55,55,55] [60,60,60,60]

Table 4.3: Sample data set for working sensors used in state flow chart

To simulate the error state initiation in the state-flow chart, a different sample set is created where one of the unlocking hall-effect sensors fails to reach it's threshold, resulting in halted further operations. This data can be observed as follows:

Sensor	Nature	Size	Time	Signal values
Proximity_sensors (threshold= 60)	uint16	[1x4]	0 1 2	[0,0,0,0] [30,30,30,30] [60,60,60,60]
Locking_sensors (threshold= 90)	uint16	[1x4]	0 1 2	[0,0,0,0] [45,45,45,45] [90,90,90,90]
Unlocking_sensors (threshold= 180)	uint16	[1x4]	0 1 2	[90,90,90,90] [135,135,135,135] [180,160,180,180]
Proximity_sensors_unload (threshold= 60)	uint16	[1x4]	0 1 2	[50,50,50,50] [55,55,55,55] [60,60,60,60]

Table 4.4: Sample data set for faulty sensor used in state flow chart

These sample data values are utilized as inputs in the state-chart for simulating transition from one state to another. In each state, appropriate outputs are generated for controlling the actuators associated with the spreader and the crane utilizing it. These output signals are used as confirmation to initiate or stop a particular actuator. These signals operate on boolean logic where a FALSE output reading is taken as a signal to stop the actuator and TRUE output reading initiates the actuator. These output parameters are enlisted as follows:

Output nomenclature	Nature	Size
Lower_spreader	Boolean	1
Lift_spreader	Boolean	1
Twist_lock	Boolean	1
Twist_unlock	Boolean	1
Reset_locks	Boolean	1
Locking_pins	Boolean	1

Table 4.5: Output data for state-flow chart in MATLAB simulink

Finally, a block diagram is created with all the defined inputs and outputs which are connected to the state flow chart as follows:

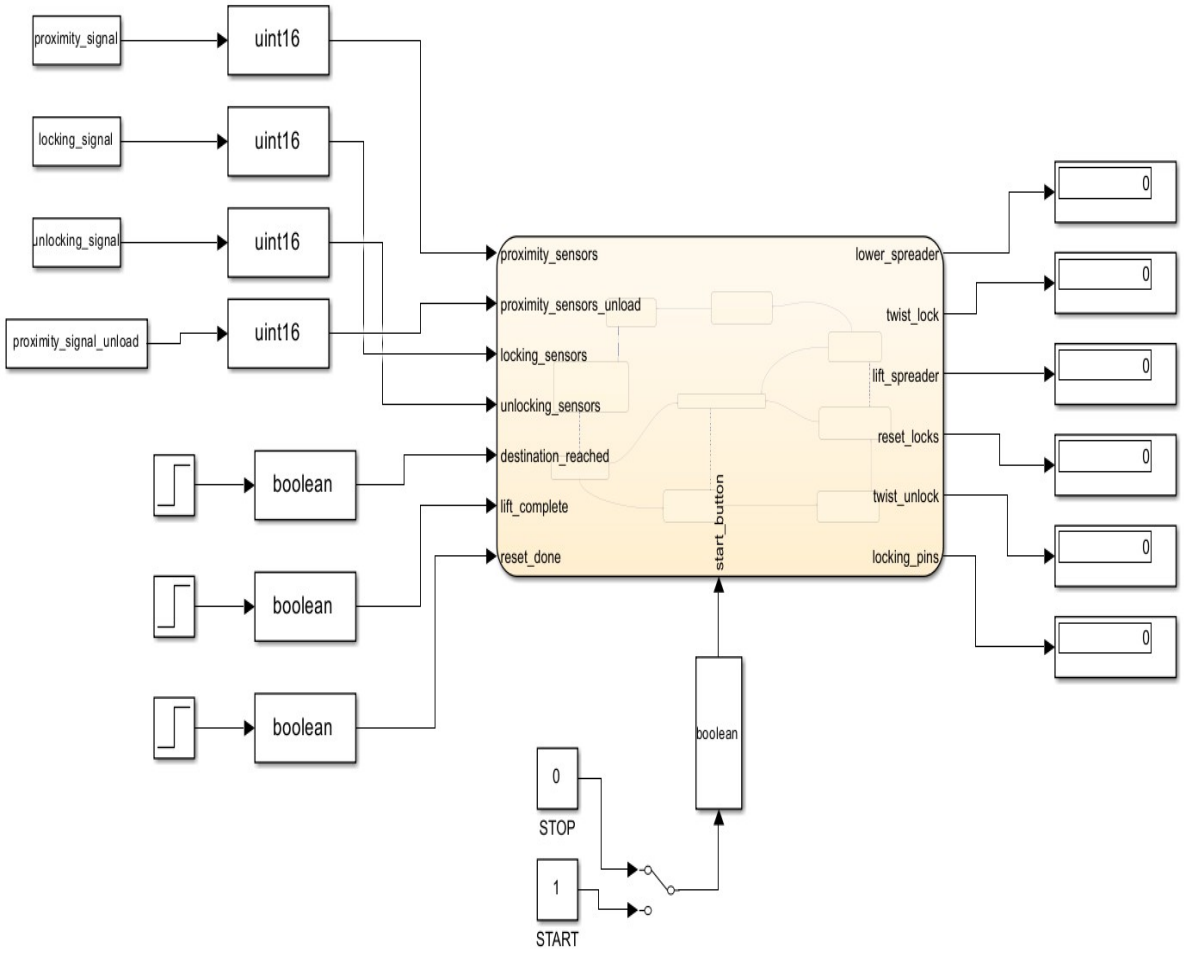

Figure 4.7: Block diagram of spreader operations

As observed from Figure 4.7, a block diagram is created in simulink to test the feasibility of the state chart. The testing is carried out in two phases, firstly to observe a successful operational cycle where all states are accessed and secondly to investigate an error state entry to verify whether the chart restricts transition to further states.

Initially, the working sample data set defined in Table 4.3 is loaded onto the workspace of MATLAB for reference. A fixed discrete-step simulation is conducted on simulink to verify the functioning of the state-flow chart. The sequence viewer function is used to observe the transition from one state to another, as follows:

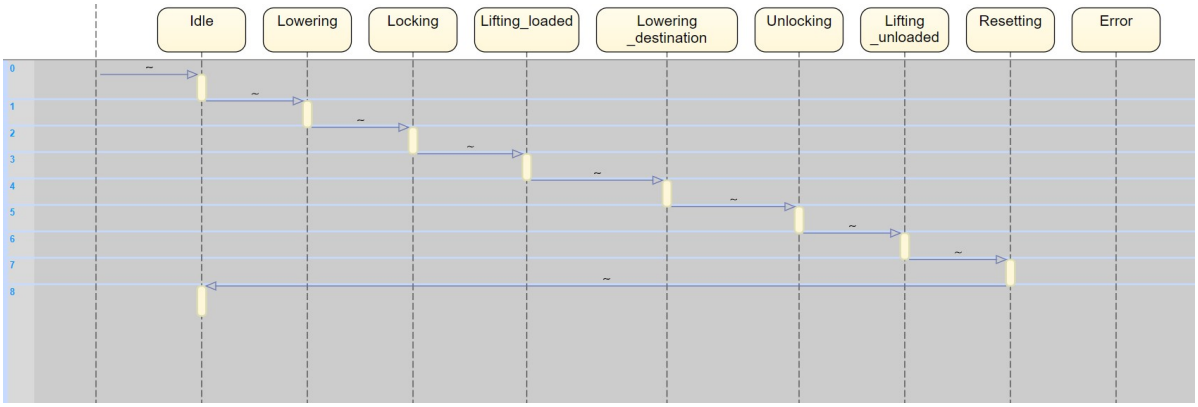

Figure 4.8: State-flow sequence chart for working operation cycle

As observed from Figure 4.8, the state-chart has successfully transitioned to each state as per its defined operational sequence and returned back to idle after completion without activating the error state. Now, let's see what happens when a faulty signal reading from Table 4.4 where one of the unlocking hall sensors provides a faulty reading gets loaded onto the workspace for simulink reference.

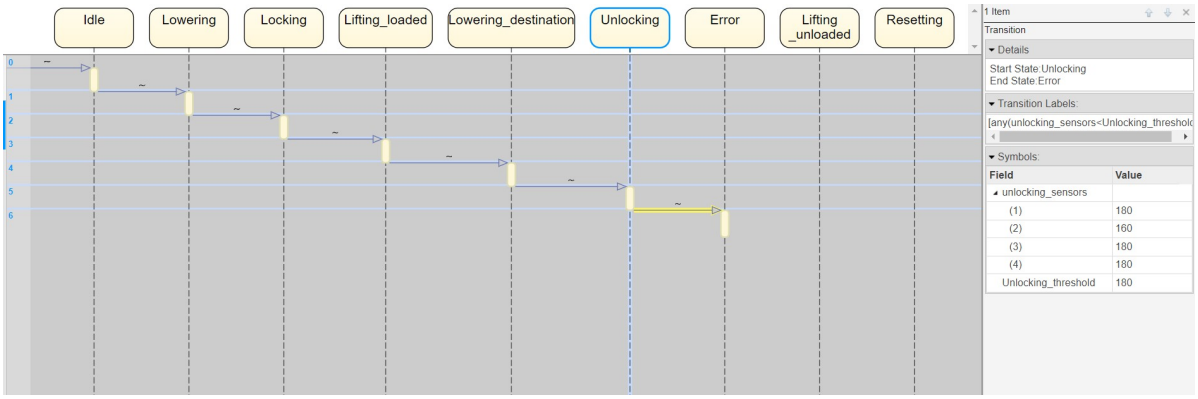

Figure 4.9: State-flow sequence chart with error state

As observed from Figure 4.9, further operations after the unlocking state are not initiated as one of the unlocking hall sensors failed to reach threshold and this consequently activates the error state. Therefore, the entire operational sequence of the state flow chart has been verified with an error state initiation. It is observed that the state transitions function appropriately and are capable of achieving automated locking/unlocking with error detection in case of faulty sensors.

4.2.3. Evaluation of operational feasibility

The chosen apparatus of actuators and sensors for twist lock handling surpass the limitations observed in current automatic spreaders, mentioned in Section 1.2. The landing pins are replaced with inductive proximity sensors which offer no-contact detection and continuous position monitoring. The use of individual stepper motors at each corner provides better control over twist lock rotation and reduces the complexity of rotating mechanism due to less number of moving parts. A suitable control algorithm is created, tested and successfully evaluated to integrate these actuators and sensors. It possesses in-built error detection which can potentially reduce the risk of damage or accidents during handling. Therefore, the iterative cycle for verifying operational feasibility is completed and the spreader design can proceed to a final product requirement verification.

4.3. Product requirement verification

The iterative cycles for verifying structural integrity and operational feasibility are now complete. As part of the iterative design process, the final iteration of the automated spreader has to be compared to the pre-defined product requirements mentioned in Section 2.2. These product requirements are verified as follows:

Dimensional feasibility: To achieve dual-size lifting in the form of TEU and FEU containers, the spreader design was split into two main components, namely the mainframe and extendable arms. Both components are dimensioned according ISO 668, the standard dictating freight container dimensions, as observed in Section 3.1. An appropriate linear actuator defined in Section 4.1 is utilized to extend the arms to facilitate FEU containers.

Load capacity: To verify that the new spreader frame is capable of handling all static and dynamic loads during it's operations, a Finite Element Analysis (FEA) is conducted where all relevant loads are applied in Section 3.2 and tested to check yielding/buckling of the structure. On observing the FEA results in Section 3.2.3, it can be confirmed that the spreader is fit for operations.

Environmental exposure: A stainless steel alloy is chosen for the spreader frame capable of handling exposure to harsh environmental conditions experienced at terminals. Moreover, the effect of winds on the spreader during operations is also accounted for during the FEA , as observed in Chapter 3. The actuators and sensors chosen for operations have specific Ingress Protection (IP) rating (65 or above) to prevent contamination caused by dust and moisture.

Safety standards verification: For a new spreader design to be acceptable for introduction in a terminal, it has to undergo a safety standard verification issued by the region in which the terminal exists. A crucial aspect of evaluating the FEA is checking the design safety standard competence and on observing the results obtained in Section 3.2.3, it is confirmed that the spreader frame is competent according to the container spreader safety standard NEN-EN 15056.

Automated twist lock handling: A finite state-machine control chart is created on MATLAB simulink for integrating the actuators and sensors required to enable automated handling of the spreader's twist locks, as observed in Section 4.2. On observing the results of the state flow-chart simulation, the chosen components and their control logic can be deemed feasible for operations.

Compatibility: The spreader utilizes a connection plate that allows quick release of the spreader along with possibility of attachment to any secondary handling equipment. The top of the plate can be modified for pulleys, hooks, slings or fixed attachment to cranes and the bottom plate has insertion slots to allow latching of the spreader extension. This allows greater compatibility along with faster replacement.

Accessibility: The design of spreader frame has been optimized for ease of access via strategic cutouts while maintaining structural integrity. The components required for operations are strategically located in the frame to allow access for maintenance or replacement.

Independent operations: The mainframe of the spreader is designed considering space allocation for installing an internal source of power. An estimate power consumption by the spreader components is calculated and a suitable source of power is investigated. It is observed that the spreader can potentially operate for 20 hours on it's independent power supply.

5. Discussions

The iterative cycles have successfully satisfied all product requirements, resulting in an enhanced spreader design. On comparison to the limitations observed in Section 1.2 regarding the current spreader assembly, following are the characteristic improvements observed by introducing the new design:

Level of Automation (LOA): The current LOA in spreader operations is observed to be at level 3, where a human is responsible for selection of decisions. The new spreader design with integrated control increases the LOA to level 8 in terms of locking/unlocking , where the computer executes all tasks in a predefined fashion and only notifies the operator in case of an error.

Downtime of operations: Currently, remote operators handle the automatic spreader operations in long shifts of 8 hours with an entitled 30 minute break. This results in a combined downtime of 1.5 hours for three shifts. Moreover, operator fatigue can introduce a risk of accidents. These issues can be solved by introducing a spreader that possesses automated twist locking with in-built error detection and continuous operational capability of 20 hours, reducing the downtime by 1 hour, as the spreader can cover two entire 8 hour shifts.

Maintenance frequency: The landing pins require frequent maintenance every 3 to 6 months due to constant stress loading and wear of mechanical components. Moreover, they cannot provide continuous monitoring of engagement between spreaders and containers. These issues are alleviated by utilizing inductive proximity sensors which provide continuous position monitoring and require maintenance only once a year for calibration as they offer no-contact detection, capable of reducing the maintenance frequency by up to 75 percent.

Mechanical complexity: The drive linkage utilized for twist lock rotation comprises of 8 moving mechanical components which increases the potential failure points. Furthermore, they cannot provide independent control over lock rotation at each corner. By utilizing steppers motors possessing a rotating shaft at every corner, the number of moving parts is reduced to just 4 and rotation at each corner of the spreader can be monitored separately, improving fault diagnosis and reducing potential failure points by 50 percent.

Mobile operations: Currently, spreaders always require an external source of power supply. This restricts the use of spreaders in mobile operations around the terminal where power supply could be limited. By introducing an in-built replaceable battery, the mobility of the spreader is improved making it more capable for independent remote operations.

In-built release mechanism: By introducing an-inbuilt quick release mechanism with an intermediate connector plate, the spreader can be quickly attached/detached from a crane during emergencies. For example, if the crane suddenly stops functioning due to loss of power supply or damage and the spreader needs to be detached as soon as possible, the in-built battery in combination with the quick release can be utilized.

5.1. Future Work

The automated spreader with an independent locking mechanism reduces dependency on remote operators and enhances container terminal automation. Future research includes developing an independent positioning system that identifies the global position of the spreader with respect to a target container. The obtained data from this positioning system can be integrated in the state flow chart to mitigate the assumptions about spreader positioning. Appropriate sensors can be introduced to identify the category of container to be transported (FEU/TEU) and integrated with the extension actuators defined in Section 4.1. To test the state chart in a more realistic setting, the sample signal datasets used for reference can be replaced by physical readings from real sensors. This can be achieved by using appropriate hardware interface techniques that allow the state chart to refer live sensor readings. For example, using Arduino/Raspberry pi to connect to the sensors and integrating it into state flow via Simulink Desktop Real-Time using the appropriate support packages. Finally, to check appropriate actuator functioning, a 3-D multi-body simulation can be created for testing one operation cycle of the spreader. Once these advancements are implemented and simulated, a fully operational prototype can be developed to evaluate real-world performance.

References

[1] Aman Chopra. Container transport contribution. https://stallionexpress.ca/blog/global-container-shipping-statistics/#:~:text=Containerization%20is%20essential%20in%20international,the%20total%20trade%20value%20worldwide, 2024. Retrieved on May 30, 2024.

[2] Martin Placek. Container throughput at ports worldwide from 2012 to 2021, with a forecast through 2027. https://www.statista.com/statistics/913398/container-throughput-worldwide/#:~:text=In%202022%2C%20global%20container%20throughput,foot%20equivalent%20units%20(TEUs)., 2024. Retrieved on May 30, 2024.

[3] Marialena Vagia, Aksel A. Transeth, and Sigurd A. Fjerdingen. A literature review on the levels of automation during the years. what are the different taxonomies that have been proposed? *Applied Ergonomics*, 53:190–202, 2016. ISSN 0003-6870. doi: https://doi.org/10.1016/j.apergo.2015.09.013. URL https://www.sciencedirect.com/science/article/pii/S0003687015300855.

[4] Tuan Le-Anh and M.B.M. De Koster. A review of design and control of automated guided vehicle systems. *European Journal of Operational Research*, 171(1):1–23, 2006. ISSN 0377-2217. doi: https://doi.org/10.1016/j.ejor.2005.01.036. URL https://www.sciencedirect.com/science/article/pii/S0377221705001840.

[5] Yu E Yezhov, IV Zub, and VL Shchemelev. The use of digital technology when positioning the spreader relative to the plane of the container. In *IOP Conference Series: Earth and Environmental Science*, volume 539, page 012167. IOP Publishing, 2020.

[6] Tandemloc. Container lift spreaders, 2018. URL https://www.tandemloc.com/container-lift-spreaders-2. Accessed: 27 December,2024.

[7] Container Technics. Instruction flyer semi-automatic spreaders, 2023. URL https://www.containertechnics.com/blog/instruction-flyer-semi-automatic-spreaders. Accessed: 27 December,2024.

[8] Cooper Handling. Fully automatic container spreader, 2021. URL https://cooperhandling.com/product/fully-automatic-container-spreader/. Accessed:27 December,2024.

[9] Ministry of Social Affairs and Employment, SZW. Working hours act, 2024. URL https://business.gov.nl/staff/terms-of-employment/working-hours-act/. Accessed: March 9, 2025.

[10] BROMMA spreaders. Bromma sts45 key functionalities animation, April 2023. URL https://youtu.be/PqJCBMfjsoQ?si=oTYu7QEPtzgpGBFd. Accessed: December 15, 2024.

[11] GBM Industry. What is container spreader for?, 2022. URL https://www.gbm-industry.com/container-spreader/. Accessed: March 9,2025.

[12] Aguedo E. Bello and John Lafitte. Purchase, operations and maintenance of a container spreader. *Port of Miami Crane management*, 2021.

[13] BROMMA. Sts spreaders. URL https://bromma.com/product-category/sts-spreaders/. Accessed: February 25, 2025.

[14] Bromma. Ssx40/ssx45, 2023. URL https://bromma.com/products/ssx40-ssx45/. Accessed: February 25, 2025.

[15] Interaction Design Foundation IxDF. Design iteration brings powerful results. so, do it again designer! *Interaction Design Foundation - IxDF*, January 2 2024. URL https://www.interaction-design.org/literature/article/design-iteration-brings-powerful-results-so-do-it-again-designer.

[16] Royal Netherlands Standardization Institute. *NEN-EN 15056: Cranes - Requirements for container handling spreaders*. NEN, 2009.

[17] International Organization for Standardization. *ISO 668:2013 - Series 1 freight containers — Classification, dimensions and ratings*. ISO, 2013. URL https://www.iso.org/standard/61988.html.

[18] Industrial Metal Supply. What is alloy steel?, 2025. URL https://www.industrialmetalsupply.com/blog/what-is-alloy-steel. Accessed: 31-Jan-2025.

[19] Andrew Clark, Gareth Hobson, Robert Combier, and Sandeep Urankar. Transforming engineering design with finite element analysis, Dec 2024. URL https://rescale.com/blog/harnessing-the-potential-of-finite-element-analysis-transforming-engineering-design-and-testing/#:~:text=FEA%20typically%20involves%20three%20main,solution%2C%20and%20post%2Dprocessing.

[20] JTEKT Corporation. Bearing trivia – 1st series: What is a bearing?, 2023. URL https://koyo.jtekt.co.jp/en/bearing-column/bearing_trivia_1st_series/bearing_trivia_1st_series_01.html. Accessed: 31-Jan-2025.

[21] Stinis. Comprehensive guide to container spreaders, 2019. URL https://www.stinis.com/comprehensive-guide-container-spreaders/. Accessed: March 2, 2025.

[22] Stinis. In-depth guide to twistlocks in container handling, 2025. URL https://www.stinis.com/in-depth-guide-to-twistlocks-in-container-handling/. Accessed: 31-Jan-2025.

[23] Royal Netherlands Standardization Institute. *NEN-EN 13001-2: Cranes – General Design – Part 2: Load Actions*. NEN, 2021.

[24] Study.com. How to calculate torque – explanation, 2025. URL https://study.com/skill/learn/how-to-calculate-torque-explanation.html. Accessed: 31-Jan-2025.

[25] Dolf Broekaart. Why should you consider performing non-linear finite element analysis?, 2015. URL https://simulation-blog.technia.com/simulation/why-should-you-consider-performing-non-linear-finite-element-analysis. Accessed: February 27, 2025.

[26] Royal Netherlands Standardization Institute. *NEN-EN 13001-3-1: Cranes – General Design – Part 3-1: Limit States and Proof of Competence of Steel Structures*. NEN, 2018.

[27] Dissemination of IT for the Promotion of Materials Science (DoITPoMS). Elastic deformation: Hooke's law and stiffness, 2018. URL https://www.doitpoms.ac.uk/tlplib/mechanical_properties/elastic.php. Accessed: March 7, 2025.

[28] International Electrotechnical Commission. Ip ratings, 2025. URL https://www.iec.ch/ip-ratings. Accessed: 2025-02-07.

[29] Mark Luciano. Pros and cons of hydraulic, pneumatic, and electric linear actuators, 2021. URL https://www.progressiveautomations.com/blogs/products/pros-cons-of-hydraulic-pneumatic-and-electric-linear-actuators. Accessed: 2025-02-07.

[30] Adam Morissette. The difference between a ball screw and a lead screw in linear actuators, 2021. URL https://www.progressiveautomations.com/blogs/how-to/the-difference-between-a-ball-screw-and-a-lead-screw-in-linear-actuators. Accessed: 2025-02-07.

[31] The Pi Hut. What's the difference between dc, servo & stepper motors?, 2019. URL https://thepihut.com/blogs/raspberry-pi-tutorials/whats-the-difference-between-dc-servo-amp-stepper-motors. Accessed: 2025-02-07.

[32] Monolithic Power Systems. Stepper motors: Basics, types, and uses, 2025. URL https://www.monolithicpower.com/en/learning/resources/stepper-motors-basics-types-uses. Accessed: 2025-02-07.

[33] Variohm. What is a position sensor?, 2020. URL https://www.variohm.com/news-media/technical-blog-archive/what-is-a-position-sensor-. Accessed: 2025-02-07.

[34] Schneider Electric. What is an inductive proximity sensor?, 2022. URL https://eshop.se.com/in/blog/post/what-is-an-inductive-proximity-sensor.html. Accessed: 2025-02-07.

[35] Electronics Tutorials. Hall effect, 2020. URL https://www.electronics-tutorials.ws/electromagnetism/hall-effect.html. Accessed: 2025-02-07.

[36] StepperOnline. Nema 34 stepper motor. URL https://www.omc-stepperonline.com/nema-34-stepper-motor?mfp=145-holding-torque-ncm[707,720,800,820,850,1200,1300]. Accessed: February 27, 2025.

[37] Telemecanique Sensors. Inductive proximity sensor xs8d1a1pbl2 - 60mm. URL https://uk.farnell.com/telemecanique-sensors/xs8d1a1pbl2/inductive-proximity-sensor-60mm/dp/2847775. Accessed: February 27, 2025.

[38] Tinytronics. 3144 hall effect switch. URL https://www.tinytronics.nl/en/sensors/magnetic-field/3144-hall-effect-switch. Accessed: February 27, 2025.

[39] Super B. Benefits of lithium batteries. URL https://www.super-b.com/en/lithium-iron-phosphate-batteries/benefits-lithium-batteries. Accessed: February 27, 2025.

[40] NKON. Eve lf304 prismatic 304ah lifepo4 3.2v a-grade stock, n.d. URL https://www.nkon.nl/en/eve-lf304-prismatic-304ah-lifepo4-3-2v-a-grade-stock.htm. Accessed: February 27, 2025.

[41] Tavotech. How a buck converter works, n.d. URL https://tavotech.com/how-a-buck-converter-works/. Accessed: February 27, 2025.

[42] Wojciech Zając, Grzegorz Andrzejewski, Kazimierz Krzywicki, and Tomasz Królikowski. Finite state machine based modelling of discrete control algorithm in lad diagram language with use of new generation engineering software. *Procedia Computer Science*, 159:2560–2569, 2019. ISSN 1877-0509. doi: https://doi.org/10.1016/j.procs.2019.09.431. URL https://www.sciencedirect.com/science/article/pii/S1877050919316370. Knowledge-Based and Intelligent Information Engineering Systems: Proceedings of the 23rd International Conference KES2019.

[43] A. Bartošek and O. Marek. Quay cranes in container terminals. *Transactions on Transport Sciences*, 6(1):9–18, 2013.

[44] Michael Greminger. Estimating the s-n curve for steel alloys, Aug 2024. URL https://blog.engineeringpaper.xyz/estimating-the-s-n-curve-for-steel-alloys.

A. Scientific research paper

Design of automated container spreader with independent locking mechanism

Authors: Jyotirmoy Jana, Chamod Wijesinghe, Dr. Jovana Jovanova
Faculty of Maritime and Transport Technology (MTT),
Delft Univeristy of Technology (TU Delft), The Netherlands

Abstract

The increasing global container trade has intensified demands on container handling technology. Automation has addressed many challenges, but limitations persist, particularly in spreader design. These attachments, equipped with rotating twist locks, rely on remote-controlled actuators and sensors. However, current designs exhibit frequent maintenance, multiple failure points, and limited sensing capabilities. Additionally, dependence on external power restricts mobility, limiting their use in smaller terminals and remote operations. This research employs an iterative design approach to develop a novel spreader that reduces maintenance frequency by 75 percent, minimizes failure points by 50 percent, and integrates an advanced control algorithm with built-in error detection. This reduces reliance on remote operators, enhancing safety by mitigating operator fatigue-induced errors. An internal power source enables 20 hours of continuous operation, while the independent control system reduces downtime by 1 hour, minimizing delays from operator breaks.
Keywords: *Container handling technology, Automation levels, Container spreaders, Automated lock handling mechanism , Reduced maintenance, Failure points, Improved mobility, safety*

Introduction

The globalization of industrial trade and the expansion of international supply chains have placed significant demands on the transportation sector, driving the adoption of standardized techniques such as containerization. Introduced in 1956, containerization, utilizing Twenty-foot Equivalent Units (TEUs) and Forty-foot Equivalent Units (FEUs), now accounts for approximately 60 percent of global trade value. In 2024, global container handling reached 901 million TEUs, with projections exceeding 1 billion TEUs in the near future [2], as observed from Figure A.1. This growth necessitates advancements in container transportation technologies, particularly in associated automation technologies.

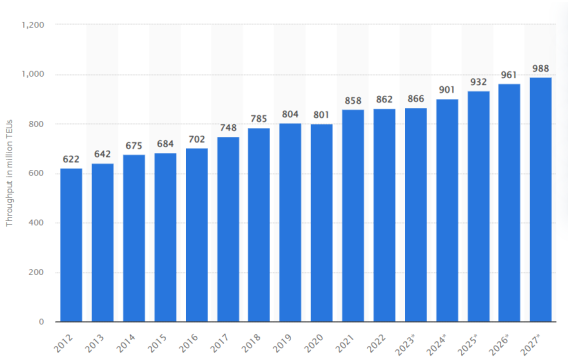

Figure A.1: Global trends of container trade

Automation in engineering involves replacing human-operated tasks with machinery, categorized into Levels of Automation (LOA) ranging from manual control (Level 1) to fully autonomous systems (Level 8) [3]. In container terminals, automation has been exemplified by introduction of equipment such as Automated Guided Vehicles (AGVs) and Rail-mounted Gantry Cranes to improve efficiency and safety [4]. However, certain tasks, such as spreader operations, remain reliant on manual oversight, limiting the potential for higher LOA. Spreader systems, critical for container handling, are classified into manual, semi-automatic, and fully automatic types:

(a) Manual spreader

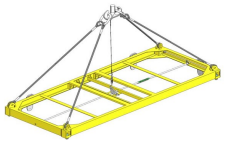

(b) Semi-automatic spreader

(c) Fully-automatic spreader

Figure A.2: Line-up of currently available container spreaders

Fully automatic spreaders, while reducing the need for on-site operators, still require remote human intervention, placing them at LOA=3. These remote operators have to endure long shifts of 8 hours with 30 minute entitled breaks, leading to downtime of spreader operations [9]. The current apparatus for twist lock handling observed in Figure A.3 faces certain limitations, such as the landing pins utilized for container detection relying on physical contact for successful detection. This imposes significant stress on the pins over repeated usage causing damage to its mechanical components, leading to frequent maintenance every 3-6 months [11]. Moreover, the actuating mechanism for rotation of twist locks consist of 8 moving parts in the form of couplers and pivot rods which are prone to failure [13]. Limit switches utilized for confirmation of container detection and lock orientation cannot provide continuous monitoring and face degradation over time [12]. Additionally, it is observed that spreaders constantly rely on an external power supply, limiting their flexibility for remote applications.

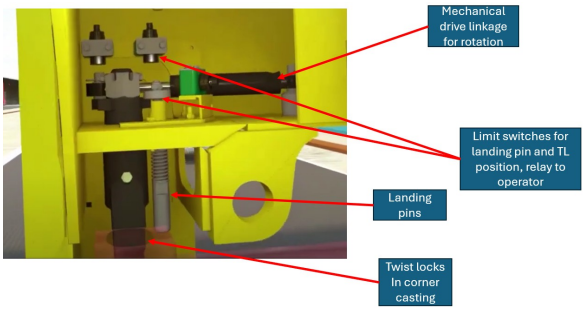

Figure A.3: Mechanism for locking/unlocking in automatic spreaders

This research proposes a enhanced spreader design addressing these limitations by integrating advanced sensors, independent corner control, and optimized frame architecture. The design aims to enhance automation levels, reduce downtime, and improve operational adaptability, contributing to the evolution of container handling technologies. A structured methodology will guide the development and evaluation of this innovative solution.

Methodology

To address the engineering challenges associated with container spreader design, a structured iterative design methodology is employed. This approach ensures continuous refinement of the design through testing and evaluation until all predefined product requirements are met [15]. The methodology is divided into four key phases: product requirements, design implementation, testing, and evaluation.

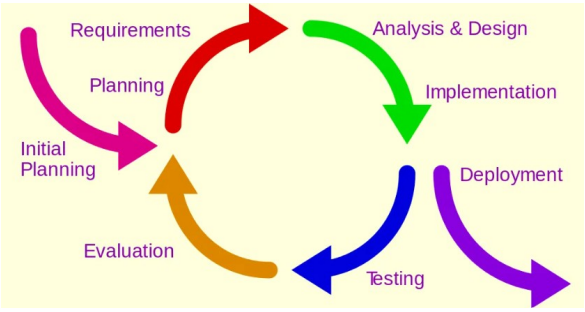

Figure A.4: Schematic of an iterative design process

The initial phase involves defining operational requirements to ensure the feasibility and functionality of the final design. These requirements serve as benchmarks for evaluating each design iteration and are tabulated as follows:

Product requirements	Explanation
Dimensional feasibility	Capable of lifting FEU and TEU containers
Load Capacity	Capable of handling all static and dynamic loads during operations
Environmental exposure	Withstand harsh winds, exposure to dust, moisture and corrosion experienced at terminals
Safety and standards compliance	Compliant to NEN EN 15056:Cranes-Requirements for container spreaders [16]
Automated locking/ unlocking	Independent locking/ unlocking mechanism
Compatibility	Easily attachable/detachable from secondary handling equipment
Accessibility	Easy access to components for maintenance/replacement
Independent operations	Space and source for internal power supply

Table A.1: Product requirements of new spreader

Based on design requirements and limitations, initial concepts include: a Split Frame Design for dual-size TEU/FEU lifting; Enhanced Load Capacity up to 40,000 kg; Steel Alloy Frame for strength, durability, and corrosion resistance [18]; and an Open Frame Design with cutouts for easy maintenance access. The design is modeled in SolidWorks, tested via FEA for structural integrity, and evaluated for operational feasibility using MATLAB Simulink. Iterative refinements ensure compliance with requirements.

Structural integrity testing

This section outlines the process for verifying the structural integrity of the optimized spreader design using Finite Element Analysis (FEA). The spreader frame consists of three main parts: the mainframe, extendable arms, and twist locks. The mainframe, sized to match a TEU container, features sliding rails for arms, housing boxes for quick-release attachments, and strategic cutouts for weight reduction and improved accessibility. Extendable arms include connection beams with guide extensions for FEU lifting and a hollow square beam at the end, housing ISO- 668 compliant twist locks made of galvanized steel for durability [17]. A rail-guide mechanism connects the mainframe and arms, while a bearing connection allows twist locks to rotate freely, secured by an actuated locking pin during transport.

To conduct a successful FEA, it is necessary to define all key parameters required for testing. These parameters include geometry and meshing, material properties, boundary conditions / constraints, acting loads and element selection. To impose the maximum stress during operations, a fully extended arm geometry is chosen with the twist locks in their locked position and meshed accordingly. Since the design of spreader frame is custom and does not use standardized beams/shells, each element is modeled as a solid body to maintain simplicity during analysis.

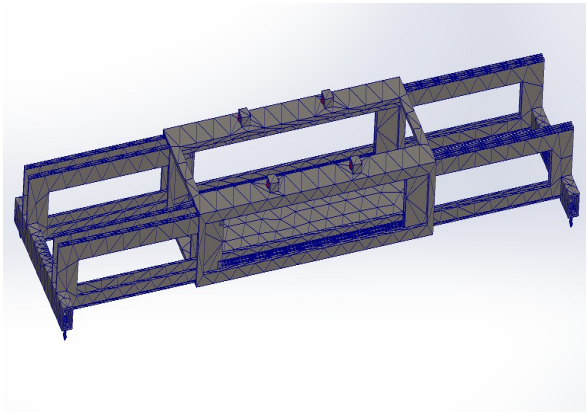

Figure A.5: Meshed spreader frame geometry

Property	Value	Units
Elastic Modulus	210000	N/mm^2
Poisson's Ratio	0.28	N/A
Shear Modulus	79000	N/mm^2
Mass Density	7700	kg/m^3
Tensile Strength	723.8256	N/mm^2
Yield Strength	620.422	N/mm^2
Thermal Expansion Coefficient	1.30E-05	/K
Thermal Conductivity	50	W/(m·K)
Specific Heat	460	J/(kg·K)

Table A.2: Material properties for spreader frame FEA

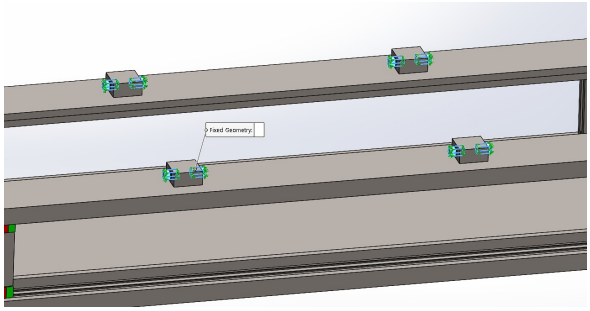

Figure A.6: Fixed geometry constraint on mainframe extensions

The acting loads on the spreader frame are calculated according to NEN EN 13001-2: Crane safety - General design - Part 2: Load actions [23]. This is the reference standard from the primary standard for container spreaders (NEN EN 15056), mentioned previously in the product requirements. The loads on the spreader include static loads, such as the container's weight acting on the twist locks during transport, and dynamic loads, primarily the inertial forces during lifting. The most significant dynamic force is the hoisting force, which occurs when transferring the container's load from the surface to the frame. This force is calculated as follows: Hoisting inertial force $= \phi *$ Container loading force
$\phi =$ dynamic hoisting factor,
assumed 1.25 according to NEN 15056
when load combination of hoisting+wind load
Therefore, the hoisting inertial force is calculated as follows: Hoisting inertial force $= 1.25 * 40000 * 9.81 = 490500N$ On each twist lock,

Hoisting inertial force $= 122,625N$

As per the product requirements, the spreader should be capable of withstanding all environmental challenges at the terminals during operations. Since container terminals are usually situated in coastal areas, they experience significant winds coming from the sea. Therefore, calculating the in-service wind forces acting on container handling equipment is crucial to verify integrity during operations. The equation provided for calculating in-service wind load is as follows:

$$F = 0.5 \cdot C_a \cdot \rho \cdot A \cdot v^2$$

where,

F is the wind force
C_a is the aerodynamic co-efficient,
assumed to be 2.4 for complex geometries
ρ is the air density, approximately
1.225 kg/m^3 at sea level
A is the projection area,
v is the wind speed,
28 (m/s) for storm winds

Transverse wind force $= 0.5 * 2.4 * 1.225 * 4.34 * 28^2 = 5002N$

Longitudinal wind force $= 0.5 * 2.4 * 1.225 * 0.73 * 28^2 = 842N$

The FEA test requires development of a scenario comprised of a combination of parameters that impose the maximum possible stress on the spreader during its operations. This scenario is observed to be hoisting a container during heavy winds, combining self-weight, hoisting inertial forces, and both wind forces. The structural integrity of the spreader frame is evaluated for this scenario using the direct solver offered by SolidWorks. There are two solver options: linear and non-linear where a linear solver assumes a linear relationship between applied loads and displacements, while a non-linear solver accounts for non-linear behavior. Typically, an initial linear analysis is conducted to assess assembly behavior before deciding whether to switch to a non-linear model. This decision depends on conditions such as material behavior (linearity under Hooke's law until yield strength is exceeded), direction of force (constant in linear analysis), direction of contact (fixed contact between components), and minor deformations (deformations should be less than 1/20th of the longest structure's length to maintain linearity) [25]. Since the spreader frame components, such as extendable arms and twist locks, remain in fixed contact via stop blocks and locking pins, the fixed contact criteria is already satisfied.

Operational feasibility testing

This section focuses on verifying the operational feasibility of the automated spreader. The process involves defining and integrating components for automated operations, developing a control algorithm, and testing the system to ensure compliance with predefined product requirements. Considering the limitations observed in the current apparatus of sensors and actuators, following recommendations are declared for components:

Arm extension actuator: Telescopic ball-screw actuators enable smooth and precise extension of the arms for FEU container lifting [29].

Twist Lock rotation actuator: Stepper motors with gear connections provide independent control over each twist lock, reducing mechanical complexity and failure points [31].

Arm position sensor: Linear encoders integrated into the actuators ensure accurate positioning of the extendable arms.

Spreader-Container engagement sensor: Inductive proximity sensors replace landing pins, enabling no-contact detection and continuous monitoring [34].

Twist Lock orientation sensor: Hall-effect sensors provide real-time no-contact feedback on twist lock positions, ensuring safe and accurate locking/unlocking [35].

The necessary sensors and actuators for spreader operations have been defined. As per the product requirements, the spreader requires an internal power supply, necessitating evaluation of power consumption for battery specifications and space allocation. Calculations are as follows:

- **Ball-screw actuator**: Each extendable arm (2700 kg) requires 3 m of extension in 20 seconds. Work done is $2700 \times 9.81 \times 3 = 79,461$ J, yielding $79,461/20 = 3,973$ W. For two actuators, total power is 7,946 W.
- **Stepper motors**: Each twist lock requires 4 Nm of torque. A NEMA 34 stepper motor operating at 48 V and 5 A consumes $48 \times 5 = 240$ W. For four motors, total power is 960 W [36].
- **Proximity sensors**: Each sensor consumes 10 mA at 24 V, requiring $24 \times 0.01 = 0.24$ W. For four sensors, total power is 0.96 W [37].
- **Hall-effect sensors**: Each sensor consumes 25 mA at 24 V, requiring $24 \times 0.025 = 0.6$ W. For eight sensors, total power is 4.8 W [38].

The total power consumption is approximately 9 kW at 48 V, requiring a discharge current of $9,000/48 = 187$ A. Lithium iron phosphate (LiFePO4) cells are chosen for their efficiency, compact size, and structural weight [39]. Each cell provides 304 Ah, 3.2 V, and weighs 5.5 kg [40]. To achieve 48 V, 15 cells are connected in series, configured as 3 rows of 5 cells. A DC buck converter steps down 48 V to 24 V for sensors [41]. The mainframe accommodates 16 packs, providing 233 kW total power. With 80% system efficiency, the spreader can operate independently for 20 hours. Depleted batteries can be replaced using a crane or lifting arm. All components for automated operation are now defined, requiring control integration for reliable functioning.

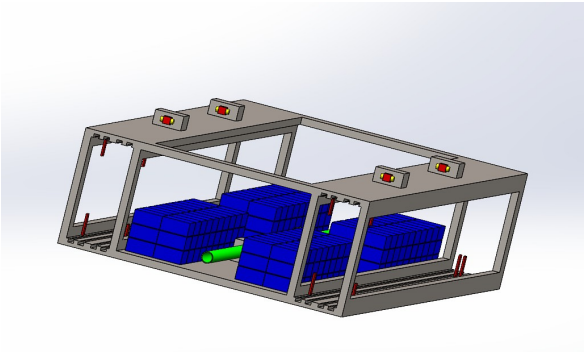

Figure A.7: Four battery packs at each corner of the mainframe

The components for automated spreader operations require an integration method to enable independent locking/unlocking. A **Finite State Machine (FSM)** control algorithm is chosen, as it operates in discrete phases, transitions based on predefined triggers, and includes an error state to halt operations during failures [42]. A state flow chart in MATLAB Simulink simulates the twist lock

handling process, broken into finite states with transitions based on sensor feedback. Assumptions include: the container type (FEU) is predefined, extendable arms are fully extended, the spreader is perfectly aligned, and lifting operations are always successful. The states and transitions are as follows:

- **Idle**: Default state awaiting user confirmation via a START/STOP switch.
- **Lowering**: Empty spreader lowers onto the container; transition occurs when proximity sensors reach their threshold.
- **Locking**: Stepper motors rotate twist locks by 90°; transition occurs when locking hall-effect sensors reach their threshold.
- **Lifting loaded**: Loaded spreader is lifted; transition occurs after a predefined time.
- **Lowering destination**: Loaded spreader lowers to destination; transition occurs when proximity sensors reach their threshold again.
- **Unlocking**: Stepper motors rotate twist locks by 180°; transition occurs when unlocking hall-effect sensors reach their threshold.
- **Lifting unloaded**: Empty spreader lifts away; transition occurs after a predefined time.
- **Resetting**: Stepper motors complete a 360° rotation to reset twist locks; transition occurs after resetting tasks.
- **Error**: Emergency state triggered if sensor values fail to meet thresholds, halting operations to prevent damage or injuries.

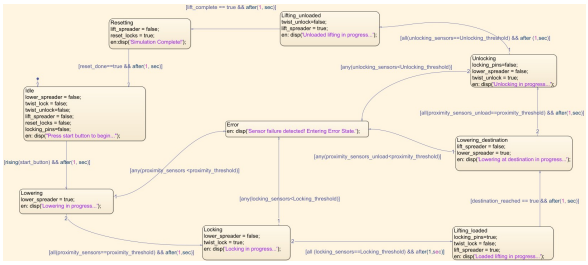

Figure A.8: State-flow chart on simulink for automated locking/unlocking

The state-flow chart transitions dependent on sensor feedback require continuous monitoring of signal values to verify if they reach predefined thresholds. A sample data set is created in MATLAB, assuming all sensors achieve their thresholds for a successful operation cycle. For instance, proximity sensors (threshold=60) transition from [0,0,0,0] to [60,60,60,60] over three time steps, while locking sensors (threshold=90) and unlocking sensors (threshold=180) follow similar patterns. To simulate an error state, a faulty data set is created where one unlocking sensor fails to reach its threshold (e.g., [180,160,180,180]), halting operations. These inputs control actuator outputs via boolean logic: TRUE initiates actions (e.g., lowering, lifting, locking, unlocking, resetting), while FALSE stops them. Output parameters include Lower_spreader, Lift_spreader, Twist_lock, Twist_unlock, Reset_locks and Locking_pins each of boolean type and size 1. The block diagram for this entire setup can be visualized as follows:

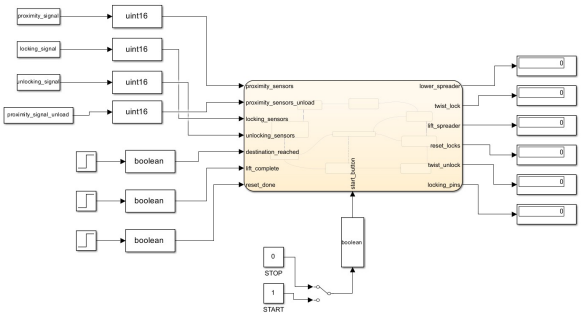

Figure A.9: Block diagram of spreader operations

The state chart implemented in MATLAB Simulink is tested in two phases to confirm the feasibility of the automated locking/unlocking logic for the spreader. First phase tests the working data set of signal reading from sensors and the second phase tests a faulty set to check whether the state chart enters the error state successfully and halts further operations.

Results

The results from both cycle tests are evaluated and compared to the product requirements to confirm whether the iteration can be concluded as final for recommendation.

Structural integrity evaluation

The post-processing stage involves visualizing and evaluating FEA results against acceptable limits defined in NEN EN 13001-3-1: Cranes - General Design - Part 3-1: Limit States and proof competence of steel structure [26]. The following physical quantities are evaluated:

1. Von-mises stress (σ_s): This stress value must be below the limit design stress (f_R), calculated as:

$$f_r = \frac{f_y}{\gamma} = \frac{620}{0.95} = 652.63\,\text{MPa}$$

From Figure A.10, the maximum von-mises stress is $\sigma_s = 251\,\text{MPa}$, proving structural competence.

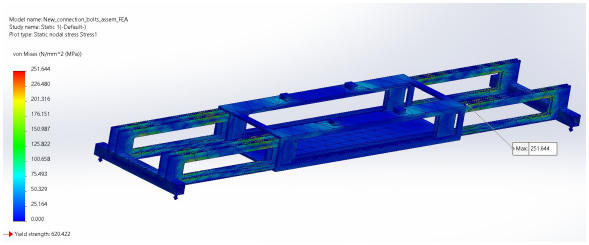

Figure A.10: FEA Hoisting case: Von mises stress

2. Factor of safety (FOS): According to NEN EN 15056, FOS must be ≥ 1.5. From Figure A.11, the observed FOS is 2.465, indicating the frame can handle 2.4 times its rated capacity.

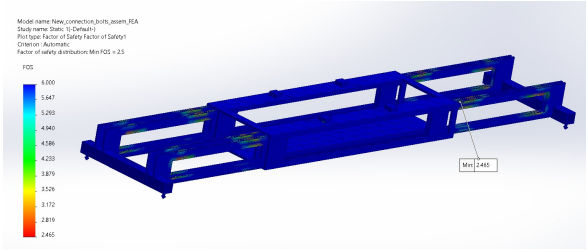

Figure A.11: FEA Hoisting case: Factor of safety (FOS)

3. Strain (ϵ): Strain must remain below the elastic limit:

$$\epsilon < \frac{361\,\text{MPa}}{210\,\text{GPa}} = 1.71 \times 10^{-3}$$

From Figure A.13, the maximum strain is $\epsilon = 8.69 \times 10^{-4}$, confirming elastic behavior.

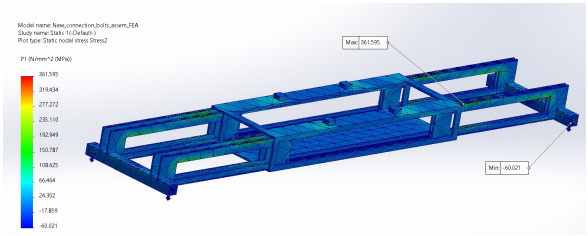

Figure A.12: FEA Hoisting case: Principle stresses

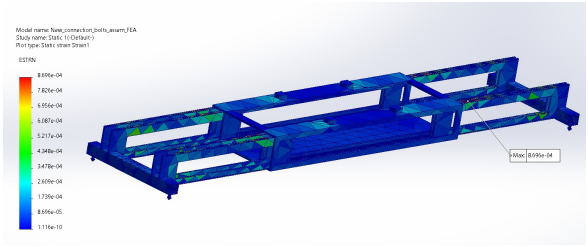

Figure A.13: FEA Hoisting case: Equivalent strain

4. Shear stress (τ): The allowable shear stress is:

$$\tau = \frac{620}{\sqrt{3} \times 1.1} = 325.41\,\text{MPa}$$

From Figure A.14, the observed shear stress is $\tau = 66.4\,\text{MPa}$, within limits.

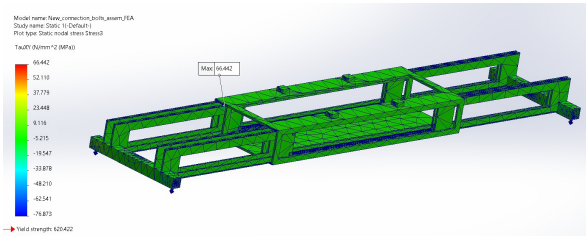

Figure A.14: FEA Hoisting case: Shear stress

5. Deflection (δ): The allowable deflection for solid cross-sections is:

$$\delta \leq \frac{12450}{200} = 62.25\,\text{mm}$$

From Figure A.15, the observed deflection is $\delta = 22.3\,\text{mm}$, within limits.

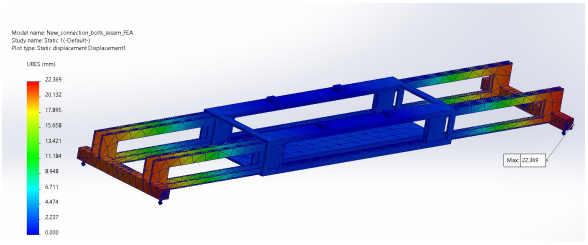

Figure A.15: FEA Hoisting case: Maximum displacement

6. Buckling (BLF): The buckling load factor must satisfy:

$$\text{BLF} = \frac{\text{Critical buckling load}}{\text{Applied axial load}} > 1$$

From Figure A.16, the BLF is 5.7, confirming structural stability.

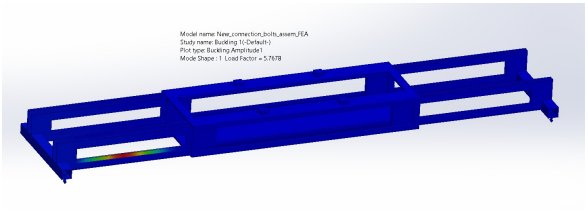

Figure A.16: FEA Hoisting case: Buckling load factor (BLF)

All evaluated quantities confirm the spreader frame's structural competence for the chosen application. The observed von-mises stress remained well below the yield strength of the chosen material. Moreover, the observed displacement of 22.3 mm is less than 1/20th of the maximum of structural length ($\frac{12450}{20} = 622.5mm$). Therefore, proceeding to a non-linear analysis is not necessary. The frame remained within allowable limits and did not yield/buckle in its test scenario and therefore can be considered feasible for operation.

Operational feasibility evaluation

Initially, the working sample data set is loaded onto the workspace of MATLAB for reference. A fixed discrete-step simulation is conducted on simulink to verify the functioning of the state-flow chart. The sequence viewer function is used to observe the transition from one state to another, as follows:

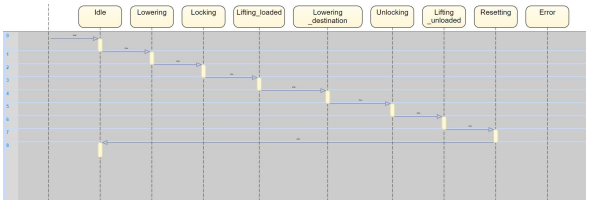

Figure A.17: State-flow sequence chart for working operation cycle

As observed from Figure A.17, the state-chart has successfully transitioned to each state as per its defined operational sequence and returned back to idle after completion without activating the error state. Now, let's see what happens when a faulty signal reading where one of the unlocking hall sensors provides a faulty reading gets loaded onto the workspace for simulink reference.

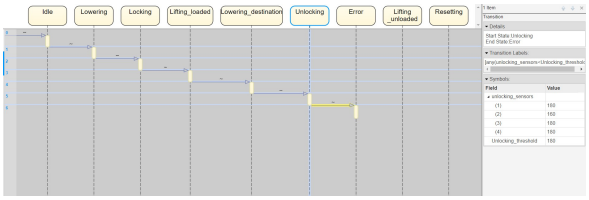

Figure A.18: State-flow sequence chart with error state

As observed from Figure A.18, further operations after the unlocking state are not initiated as one of the unlocking hall sensors failed to reach threshold and this consequently activates the error state. Therefore, the entire operational sequence of the state flow chart has been verified with an error state initiation. It is observed that the state transitions function appropriately and are capable of achieving automated locking/unlocking with error detection in case of faulty sensors.

Discussions

The iterative cycles have successfully satisfied all product requirements, resulting in an enhanced spreader design with significant improvements over current systems. The level of automation (LOA) increases from level 3 (human decision-making) to level 8, enabling fully automated locking/unlocking with error notification. Downtime is reduced by 1 hour, as the new design supports 20 hours of continuous operation, covering two full 8-hour shifts compared to the current 1.5 hours of downtime across three shifts. Maintenance frequency is cut by 75% through the use of inductive proximity sensors, which require calibration only once a year instead of the 3-6 months needed for landing pins. Mechanical complexity is reduced by replacing drive linkages with 8 moving parts with stepper motors featuring only 4 moving parts, lowering failure points by 50% and enabling independent corner rotation. The addition of an in-built replaceable battery eliminates external power dependency, enhancing mobility for remote operations. Furthermore, an in-built quick-release mechanism with a connector plate allows rapid detachment during emergencies, improving operational flexibility and safety. These advancements address current limitations, enhancing efficiency, safety, and operational capability.

Future Work

The automated spreader with an independent locking mechanism reduces dependency on remote operators and enhances container terminal automation. Future research includes developing an independent positioning system that identifies the global position of the spreader with respect to a target container. The obtained data from this positioning system can be integrated in the state flow chart to mitigate the assumptions about spreader positioning. Appropriate sensors can be introduced to identify the category of container to be transported (FEU/TEU) and integrated with the extension actuators. To test the state chart in a more realistic setting, the sample signal datasets used for reference can be replaced by physical readings from real sensors. This can be achieved by using appropriate hardware interface techniques that allow the state chart to refer live sensor readings. For example, using Arduino/Raspberry pi to connect to the sensors and integrating it into state flow via Simulink Desktop Real-Time using the appropriate support packages. Finally, to check appropriate actuator functioning, a 3-D multi-body simulation can be created for testing one operation cycle of the spreader. Once these advancements are implemented and simulated, a fully operational prototype can be developed to evaluate real-world performance.

B. Appendix

Iterative cycle for structural integrity

In addition to the physical quantities referred for verifying proof of competence of spreader in Section 3.2.3, a fatigue life analysis is conducted which estimates how much damage a structure will experience in it's expected life-span under cyclic loading. This is calculated using Palmgren-Miner's rule of cumulative damage. This value is calculated as follows:

$$d = \sum_{i=1}^{k} \frac{n}{N} < 1$$

where k= number of amplitude levels, n = number of life-time cycles, N= number of cycles to failure. The amplitude levels can be classified as scenarios of full-loaded containers, Half-loaded containers and empty containers carried by the spreader. However, to simulate maximum damage, only the full-load amplitude level is considered (k=1). To calculate the number of cycles the spreader will go through in it's lifetime, it is necessary to evaluate the expected yearly operation cycles along with the life-span of spreader. The number of life-time cycles can be calculated as follows:

$$n = \text{Yearly cycles} * \text{Expected life span}$$

The yearly cycles are calculated by multiplying the cycles completed per hour by the number of operating hours per day with the number of operating days per year. Currently, automatic spreaders are capable of handling up to 40 containers per hour [43]. Let's assume an 8 hour daily shift for 250 days of operations. This results in a yearly cycle value of 80,000 cycles. The expected life-span of the spreader is assumed to be 10 years. This provides a lifetime cycle value of:

$$n = 80,000 * 10 = 800,000 cycles$$

A S-N curve is utilized to calculate the number of cycles to failure. This curve compares the range of alternating stress values to the number of cycles to failure. The stress range is the difference between the maximum and minimum normal stress values. The S-N curve data for stainless steel alloy is obtained by referring to the research conducted by Greminger, where the author has attempted to plot a realistic curve according to various relevant factors [44]. Following is the S-N curve implemented in SolidWorks for fatigue analysis:

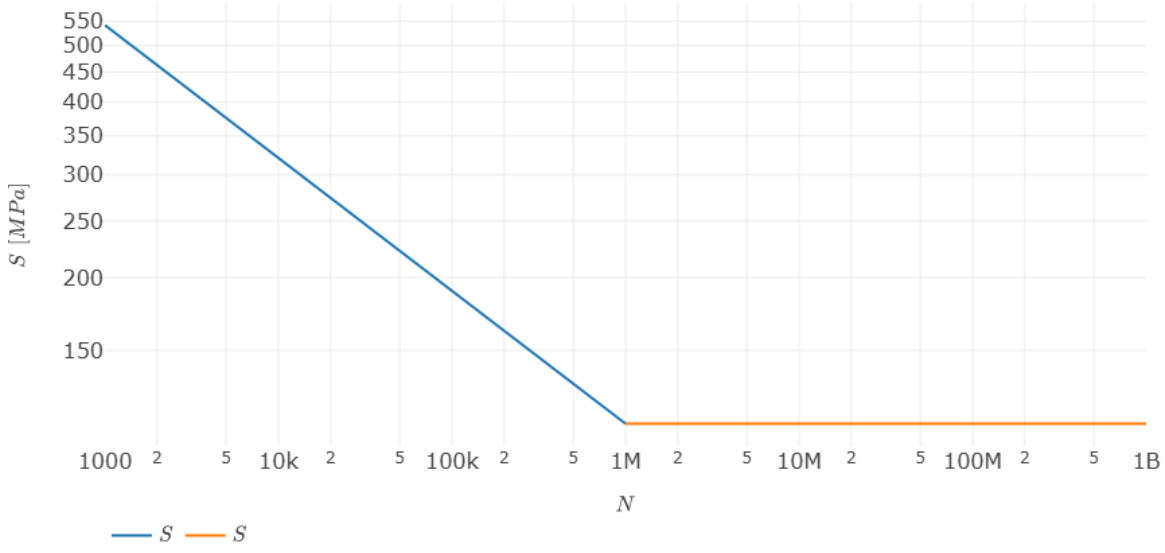

Figure B.1: Stainless steel: S-N curve

SolidWorks simulates the fatigue in terms of percentage damage for a pre-defined lifetime operating cycles. The percentage value can be interpreted as the overall cumulative damage experience during the expected life-span of the equipment.

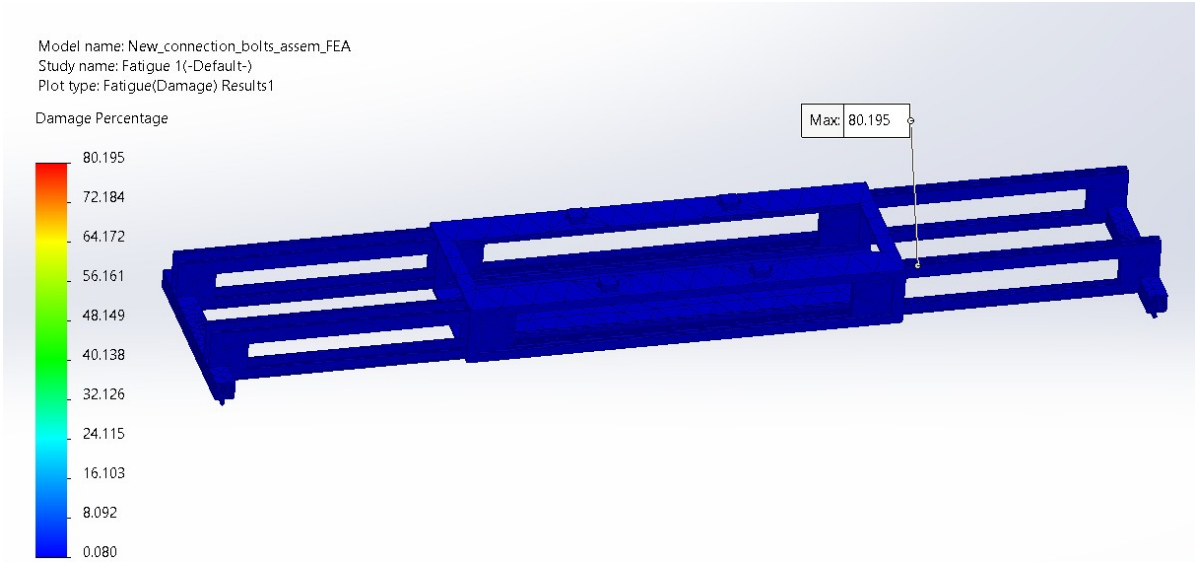

Figure B.2: FEA: total damage percentage

As observed in Figure B.2, the total damage percentage observed on the spreader during it's life of 800,000 cycles was 80 percent, which translates to a cumulative damage of 0.8. It satisfies the design standard meaning that the spreader will not experience fatigue failure in it's expected life span of 10 years.

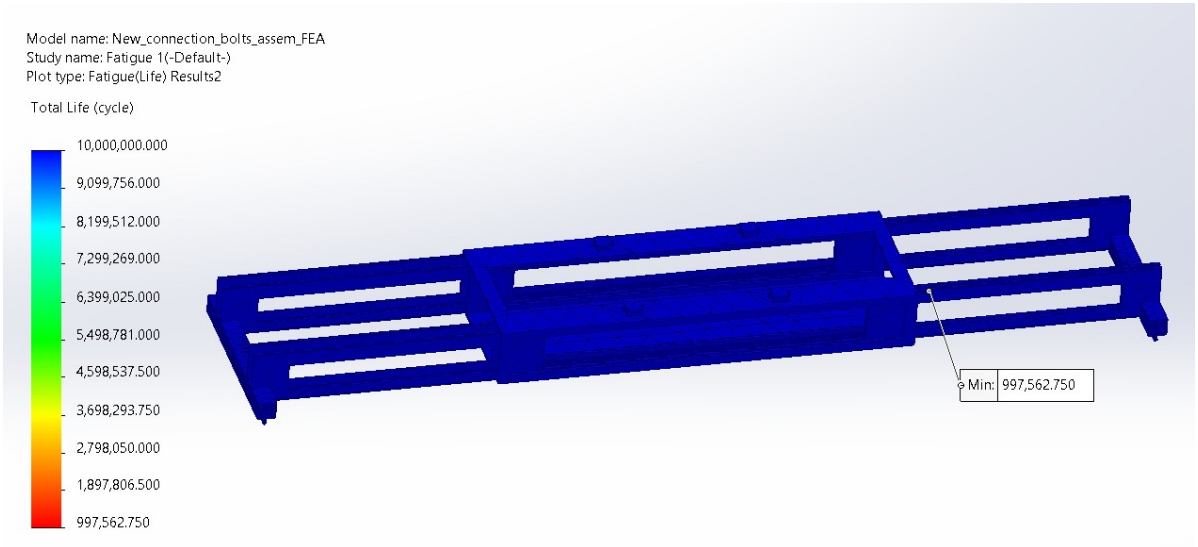

Figure B.3: FEA: fatigue life of the spreader

The spreader is expected to undergo 997,562 loading cycles before experiencing fatigue failure in it's structure, giving it an estimate fatigue life of 12.4 years based on 80,000 yearly cycles.

Iterative cycle for operational feasibility

In addition to the state-flow chart created in MATLAB simulink for automated locking/unlocking, a pseudo-code is generated on MATLAB where states are defined as cases along with initial values and thresholds of all relevant sensors required for operations. This code utilizes switch case function to transition from one state to another if all the sensor values reach their threshold. Additionally, if any sensor fails to reach it's threshold, an error state transition is introduced where all further operations are halted.

```
%% Define states
states = {'Idle', 'LoweringSpreader', 'RotatingTwistLocks_Locking', ...
          'LiftingLoadedSpreader', 'LoweringSpreader_Unlocking', ...
          'RotatingTwistLocks_Unlocking', 'LiftingSpreaderAway', 'ResettingSystem',
              'ErrorState'};

%% Initialize current state
currentState = 'Idle';

%% Initialize sensor values, thresholds and initial conditions
AllProximitySensors = [0; 0; 0; 0]; % 4x1 array for sensors at each corner
AllHallSensors_Locking = [0; 0; 0; 0]; % 4x1 array for sensors at each corner
AllHallSensors_Unlocking = [90; 90; 90; 90]; % Start unlocking hall sensor reading at 90
    degrees
Proximity_Threshold = 60; % Proximity sensor threshold (stop lowering when all sensors show
    60 mm distance from container)
DesiredOrientation_Locking = 90; % Desired twist lock angle for Locking Hall sensor
DesiredOrientation_Unlocking = 180; % Desired twist lock angle for Unlocking Hall sensor
SpreaderAtTargetLocation = false;
SpreaderClear = false;
ResetComplete = false;

%% Operator can start the operation ( can replace with positioning system feedback later )
StartOperation = input('Start operation? (1 for Yes, 0 for No): ');
if StartOperation ~= 1
    disp('Operation not started. Exiting...');
    return;
end

%% State machine logic
operationComplete = false;
while ~operationComplete
    switch currentState
        case 'Idle'
            disp('Current State: Idle');
            currentState = 'LoweringSpreader';

        case 'LoweringSpreader'
            disp('Current State: Lowering Spreader');
            AllProximitySensors = AllProximitySensors + 20;
            disp(['Proximity Sensor Values: ', num2str(AllProximitySensors')]);
            if any(AllProximitySensors < 0)
                currentState = 'ErrorState';
            elseif all(AllProximitySensors >= Proximity_Threshold)
                disp('Lowering stopped: All proximity sensors met their threshold.');
                currentState = 'RotatingTwistLocks_Locking';
            else
                disp('Lowering spreader...');
                pause(1);
            end

        case 'RotatingTwistLocks_Locking'
            disp('Current State: Rotating Twist Locks (Locking)');
            AllHallSensors_Locking = AllHallSensors_Locking + 30;
            disp(['Hall Sensor Values (Locking): ', num2str(AllHallSensors_Locking')]);
            if any(AllHallSensors_Locking < 0)
                currentState = 'ErrorState';
            elseif all(AllHallSensors_Locking >= DesiredOrientation_Locking)
                disp('Twist lock rotation stopped: All locking sensors confirm orientation.')
                currentState = 'LiftingLoadedSpreader';
            else
                disp('Rotating twist locks for locking...');
                pause(1);
            end

        case 'LiftingLoadedSpreader'
```

```
            disp('Current State: Lifting Loaded Spreader');
            SpreaderAtTargetLocation = true;
            disp('Spreader reached target location.');
            currentState = 'LoweringSpreader_Unlocking';

        case 'LoweringSpreader_Unlocking'
            disp('Current State: Lowering Spreader (Unlocking)');
            if all(AllProximitySensors >= Proximity_Threshold)
                AllProximitySensors = [40; 40: 40; 40];
                disp(['Proximity Sensor Values Dropped: ', num2str(AllProximitySensors')]);
                pause(1);
            end
            AllProximitySensors = AllProximitySensors + 5;
            disp(['Proximity Sensor Values Rising: ', num2str(AllProximitySensors')]);
            if any(AllProximitySensors < 0)
                currentState= 'ErrorState';
            elseif all(AllProximitySensors >= Proximity_Threshold)
                disp('Lowering stopped: All proximity sensors met their threshold.');
                currentState = 'RotatingTwistLocks_Unlocking';
            else
                disp('Lowering spreader for unlocking...');
                pause(1);
            end

        case 'RotatingTwistLocks_Unlocking'
            disp('Current State: Rotating Twist Locks (Unlocking)');
            AllHallSensors_Unlocking = AllHallSensors_Unlocking + 30;
            disp(['Hall Sensor Values (Unlocking): ', num2str(AllHallSensors_Unlocking')]);
            if any(AllHallSensors_Unlocking < 0)
                currentState = 'ErrorState';
            elseif all(AllHallSensors_Unlocking >= DesiredOrientation_Unlocking)
                disp('Twist lock rotation stopped: All Unlocking sensors confirm
                    orientation.')
                currentState = 'LiftingSpreaderAway';
            else
                disp('Rotating twist locks for unlocking...');
                pause(1);
            end

        case 'LiftingSpreaderAway'
            disp('Current State: Lifting Spreader Away');
            SpreaderClear = true;
            disp('Spreader is clear of the container.');
            currentState = 'ResettingSystem';

        case 'ResettingSystem'
            disp('Current State: Resetting System');
            disp('Rotating twist locks to original position...');
            pause(1);
            AllProximitySensors = [0; 0; 0; 0];
            AllHallSensors_Locking = [0; 0; 0; 0];
            AllHallSensors_Unlocking = [90; 90; 90; 90];
            SpreaderAtTargetLocation = false;
            SpreaderClear = false;
            ResetComplete = true;
            disp('System reset complete.');
            operationComplete = true;
            currentState = 'Idle';

        case 'ErrorState'
            disp('Current State: Error State');
            disp('Halting further operations due to sensor failure.');
            return;

        otherwise
            error('Invalid state');
    end
end

disp('Operation completed successfully.');
```

On compiling and running, this code can provide a step-by-step guideline on the functioning of the state-machine logic. It will not enter the error state since all sensor values are programmed to reach their threshold. To observe an error state entry, one of the sensors in the case ' LoweringSpreader_Unlocking' is forced produce a faulty reading. To observe the error state in the command window, replace the code only for this case with the following and compile again:

```
        case 'LoweringSpreader_Unlocking'
            disp('Current State: Lowering Spreader (Unlocking)');

            % Simulate a faulty sensor
            faultySensorIndex = 2; % Sensor 2 is faulty
            faultySensorValue = 50; % Stuck at this value

            % Update all sensors except the faulty one
            for i = 1:length(AllProximitySensors)
                    if i == faultySensorIndex
                        AllProximitySensors(i) = faultySensorValue; % Keep the faulty sensor
                            stuck
                    else
                        AllProximitySensors(i) = min(AllProximitySensors(i) + 20,
                            Proximity_Threshold); % Update other sensors
                    end
            end

            disp(['Proximity Sensor Values: ', num2str(AllProximitySensors')]);

            if all(AllProximitySensors >= Proximity_Threshold)
                disp('Lowering stopped: All proximity sensors met their threshold.');
                currentState = 'RotatingTwistLocks_Unlocking';
            else
                if AllProximitySensors(faultySensorIndex) < Proximity_Threshold
                    disp(['Error: Sensor ', num2str(faultySensorIndex), ' is faulty and
                        stuck at ', num2str(faultySensorValue)]);
                    currentState = 'ErrorState';
                else
                    disp('Lowering spreader for unlocking...');
                    pause(1);
                end
            end
```